Supporting information for

Non-canonical function of a small-molecular virulence factor coronatine against plant immunity: An *In vivo* Raman imaging approach

Minoru Ueda,[a] Syusuke Egoshi,[a] Kosuke Dodo,[b,c,d] Yasuhiro Ishimaru,[a] Hiroyuki Yamakoshi,[b] Takeshi Nakano,[c, e] Yousuke Takaoka,[a] Shinya Tsukiji,[f] Mikiko Sodeoka[b, c, d]

[a]Department of Chemistry, Tohoku University, 6-3 Aramaki-Aza Aoba, Aoba-ku, Sendai 980-8578, Japan
[b]Synthetic Organic Chemistry Laboratory, RIKEN, Hirosawa, Wako, Saitama 351-0198, Japan
[c]RIKEN Center for Sustainable Resource Science, Hirosawa, Wako, Saitama 351-0198, Japan
[d]AMED-CREST, Japan Agency for Medical Research and Development, Wako, Saitama 351-0198, Japan
[e]Core Research for Evolutional Science and Technology (CREST), Japan Science and Technology Agency (JST), Kawaguchi, Saitama 332-0012, Japan.
[f]Frontier Research Institute for Materials Science (FRIMS), Department of Life Science and Applied Chemistry, Department of Nanopharmaceutical Sciences, Nagoya Institute of Technology, Gokiso-cho, Showa-ku, Nagoya 466-8555, Japan.

Table of Contents:

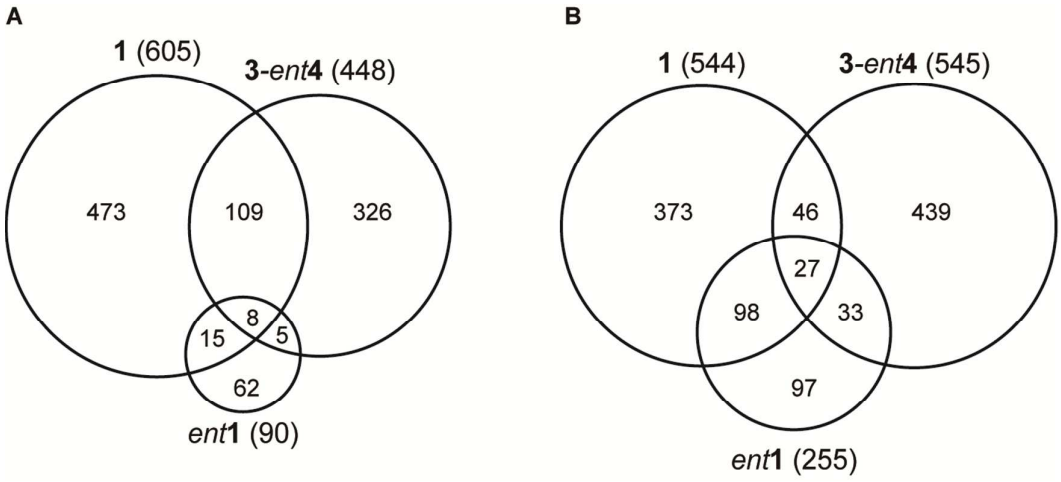

Figure S1. **Venn diagram showing the overlap genes detected microarray analysis**

(A) The numbers of upregulated gene expressions (more than twofold) by the treatment with **1**, *ent***1** or **3**-*ent***4**, compared to mock treatment are presented (**1**, *ent***1** or **3**-*ent***4** respectively). (B) The numbers of downregulated gene expressions (more than twofold) with **1**, *ent***1** or **3**-*ent***4**, compared to mock treatment are presented (**1**, *ent***1** or **3**-*ent***4** respectively).

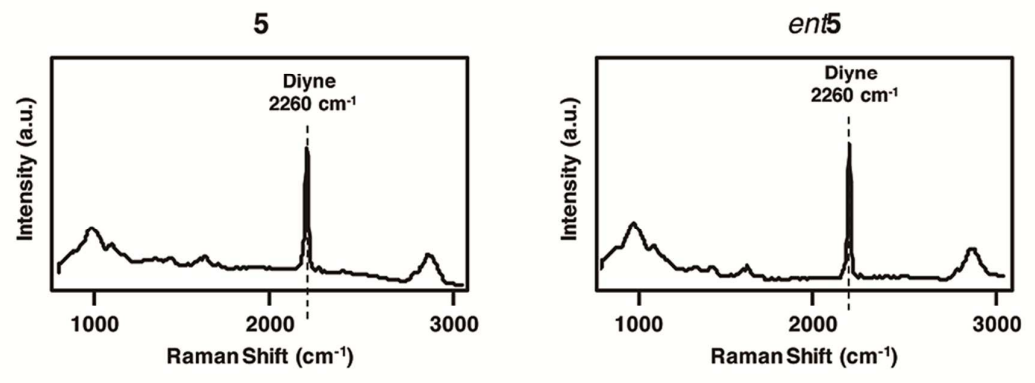

Figure S2. **Diyne Raman signal of 5 and *ent*5**.

Averaged Raman spectra of **5** and ***ent*5** as crystal forms. The light intensity at the sample plane was calculated as 6.2 mW/μm^2 from the ratio of the measured laser power between the sample position and the area of the illumination line. The exposure time for each line was 10 s.

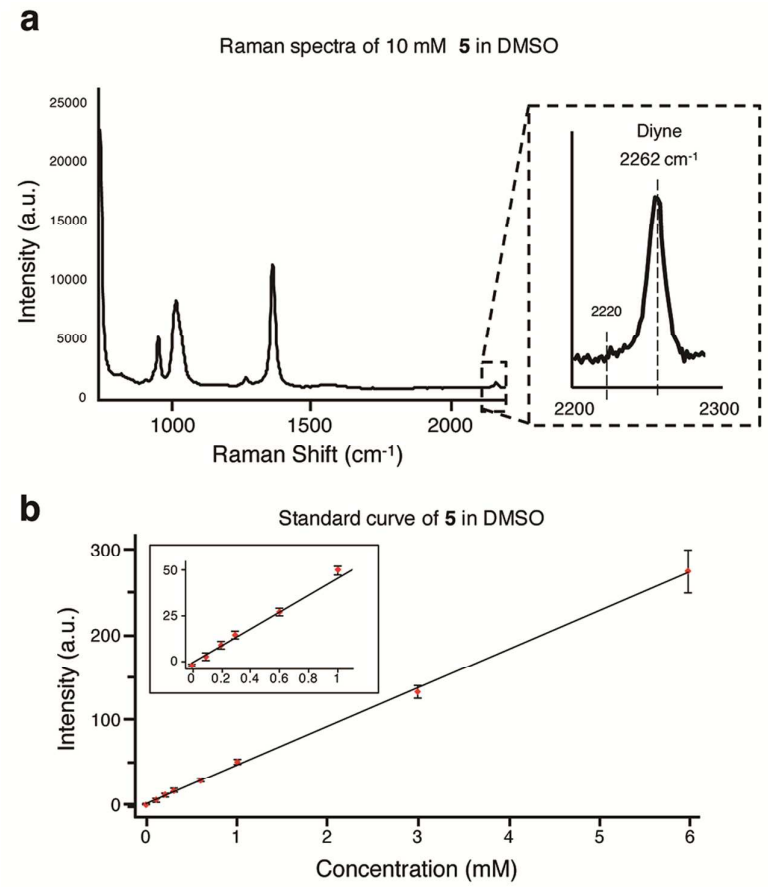

Figure S3. **Diyne Raman signal of 10 mM of 5 in DMSO (a) and Standard curve for estimation of concentration (b).**

The light intensity at the sample plane was calculated as 6.0 mW/μm^2 from the ratio of the measured laser power between the sample position and the area of the illumination line. The exposure time for each line was 120 s. (**a**) The averaged Raman spectrum obtained from 1×9 pixel region of the DMSO solution of diyne **5**. Sample concentration was 10 mM. (**b**) Standard curve for estimation of concentration. The plotted intensity was based on the peak height calculated by subtracting the background at 2220 cm^{-1} from the peak intensity at 2262 cm^{-1} and averaged from a 9×1 pixel region of the DMSO solution of diyne **5**. Bars represent mean and SE (n = 4).

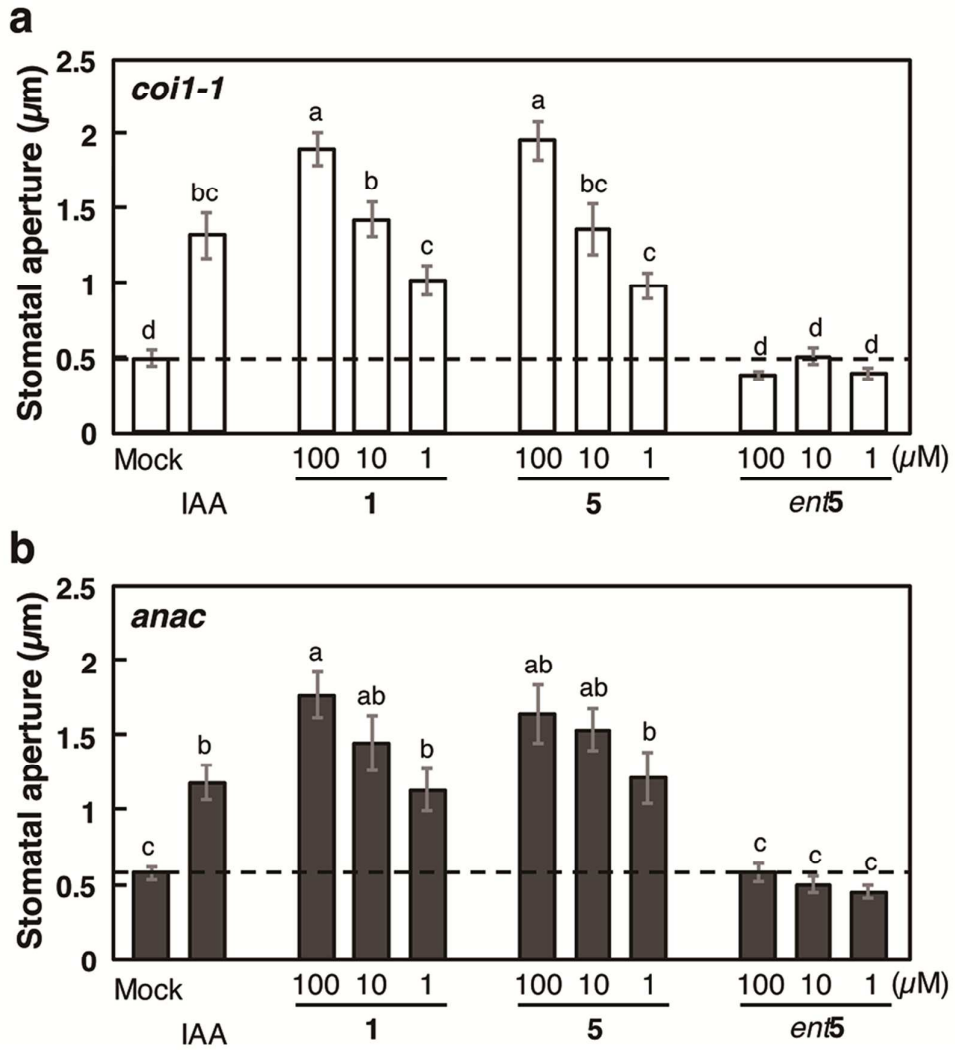

Figure S4. **Effects of 1, 5, and *ent*5 on stomatal reopening using closed stomata of *coi1-1* (a) and *anac* (b).**

IAA was used as a positive control. Dashed line indicates the mean stomatal aperture in the control experiment without test compound in which *Arabidopsis* leaf peels with closed stomata were incubated in MES buffer (pH 6.2) containing 2% EtOH. Bars represent the mean stomatal aperture with SE (n = 20 stomata). Different letters indicate significant differences between means (ANOVA: $P < 0.05$).

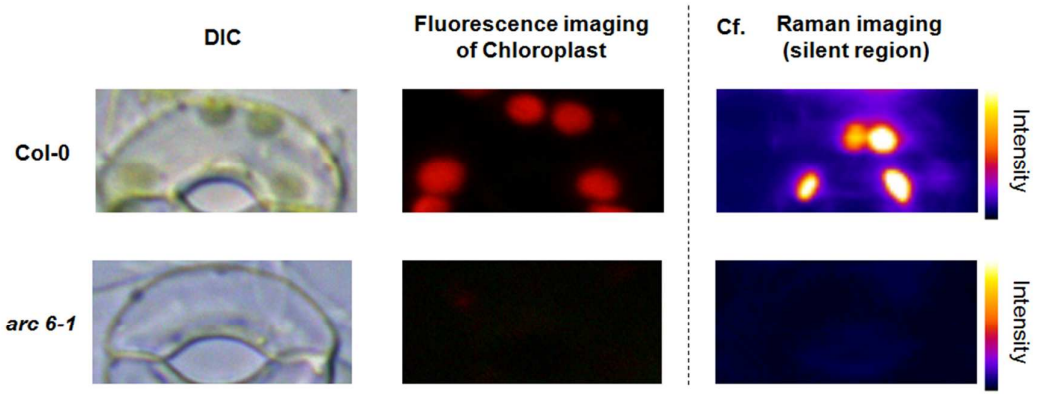

Figure S5. **Low background autofluorescence from chloroplast was observed for *arc-6* guard cell.**

DIC images (left), fluorescence images of chloroplast (>510 nm with 460-495 nm excitation light, center), and background Raman images (average of silent region: 1985-2315 cm^{-1}, right) of *A. thaliana* wild-type (Col-0) and *arc6-1*.

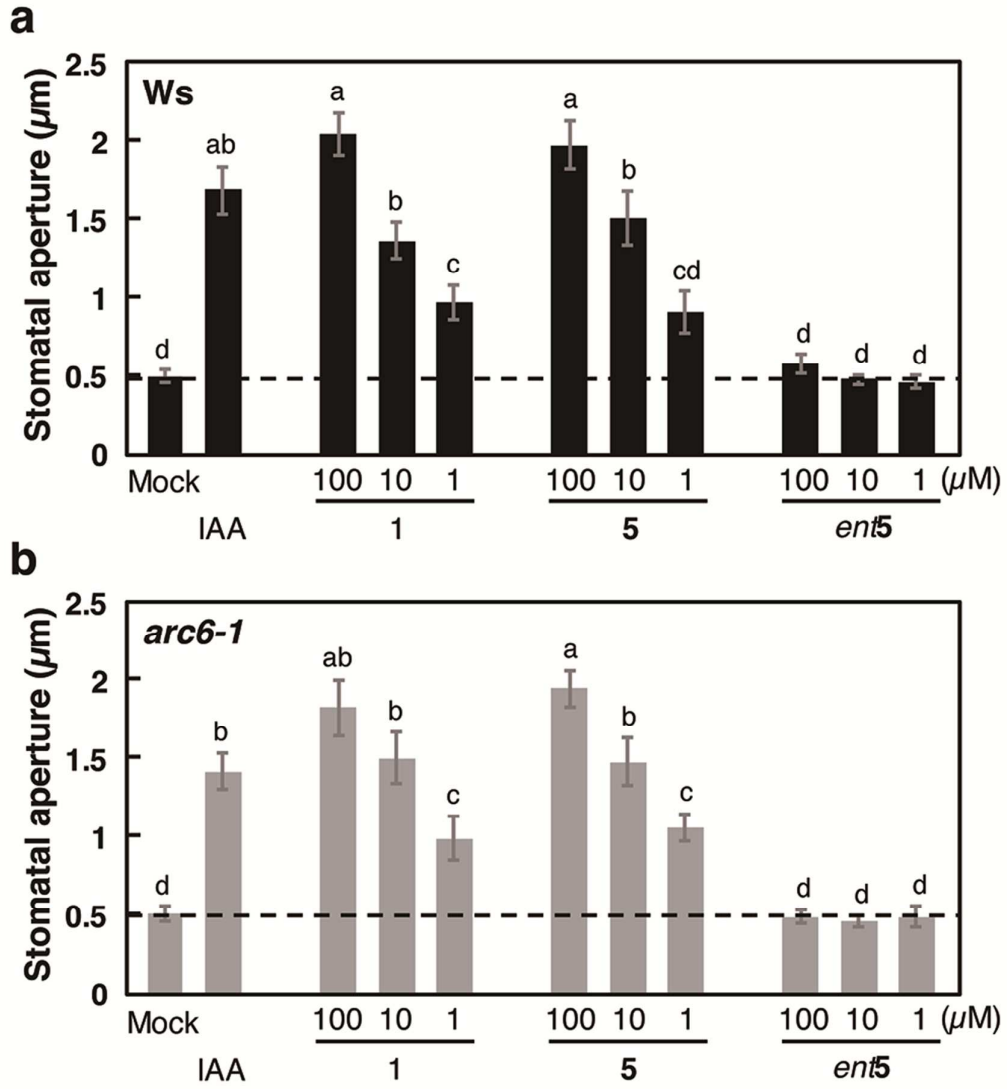

Figure S6. **Effects of 1, 5, and *ent*5 on stomatal reopening using closed stomata of Ws (a) and *arc6-1* (b) under dark.**

IAA was used as a positive control. Dashed line indicates the mean stomatal aperture in the control experiment without test compound. Bars represent the mean stomatal aperture with SE (n = 20 stomata). Different letters indicate significant differences between means (ANOVA: $P < 0.05$).

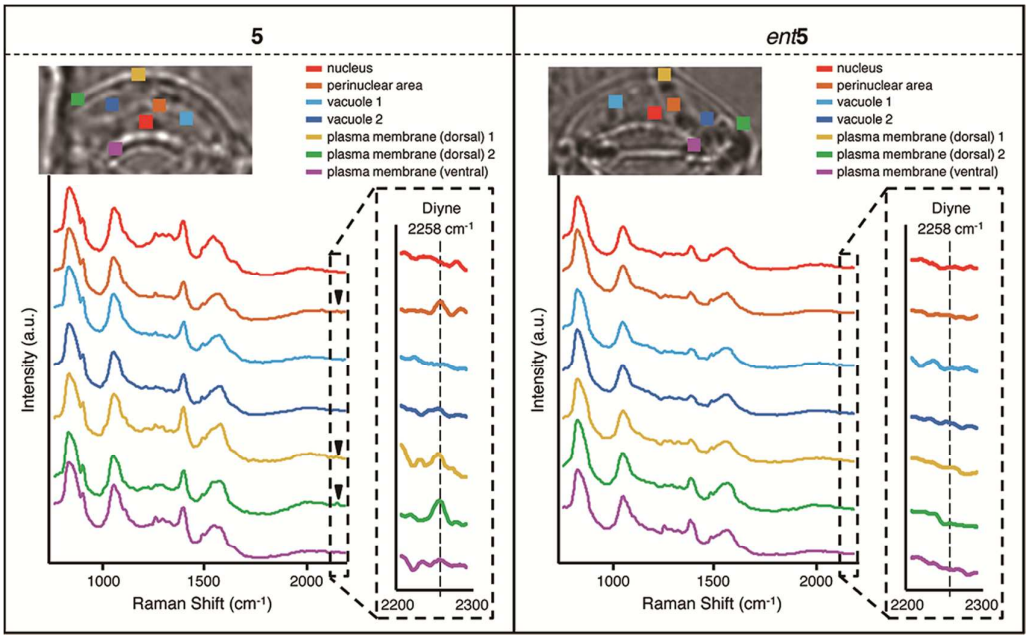

Figure S7. Raman spectra in each area of *arc6* guard cell indicating subcellular localization of 5.

Raman spectra in living guard cells of *arc6-1* were obtained after 3-hour treatment by 100 μM **5** (left)/*ent***5** (right). Averaged Raman spectra were presented for each subcellular area (1.2 μm× 1.1 μm: 3 × 3 = 9 pixels), nuclear region in red, perinuclear region in orange, vacuole in cyan or blue, plasma membrane (dorsal) in yellow or green and plasma membrane (ventral) in purple of the guard cell. The light intensity at the sample plane was calculated as 6.2 mW/μm^2 from the ratio of the measured laser power between the sample position and the area of the illumination line. The exposure time for each line was 120 s. Spectra were vertically offset for ease viewing.

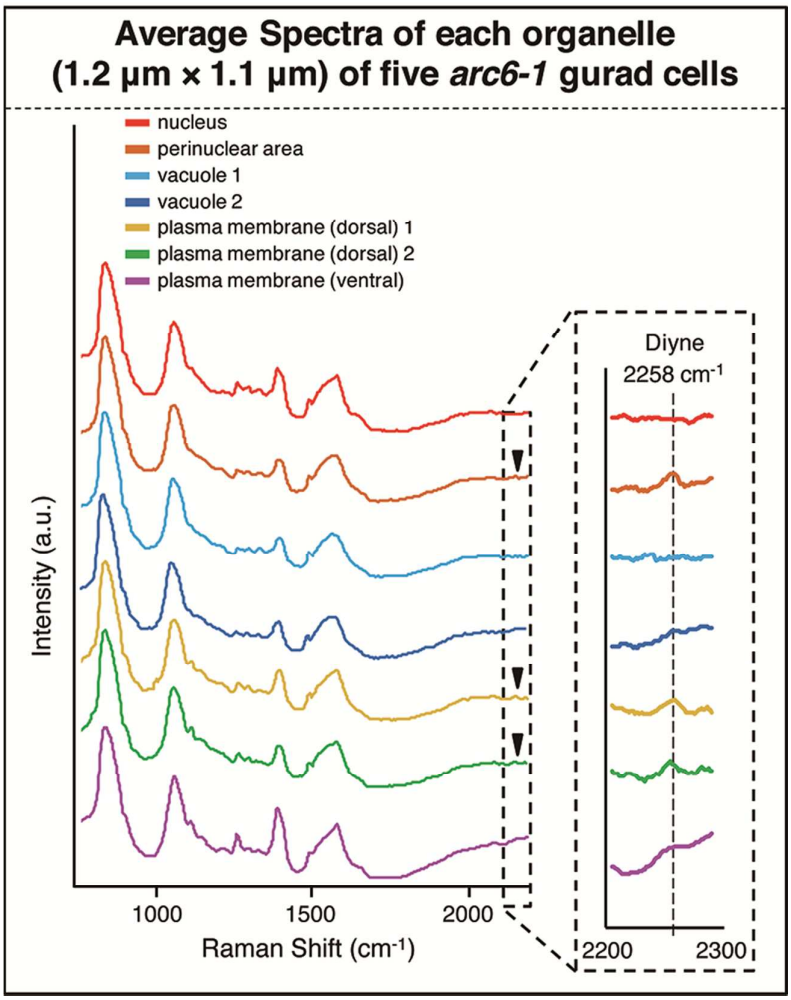

Figure S8. **Statistical analysis of five *arc6-1* guard cells treated with 5**

Average Raman spectra of each organelle region (1.2 μm × 1.1 μm: 3 × 3 = 9 pixels) of five *arc6-1* guard cells treated with 100 μM of **5**. The light intensity at the sample plane was calculated as 6.0-6.2 mW/μm^2 from the ratio of the measured laser power between the sample position and the area of the illumination line. The exposure time for each line was 120 or 150 s. Spectra were vertically offset for ease viewing.

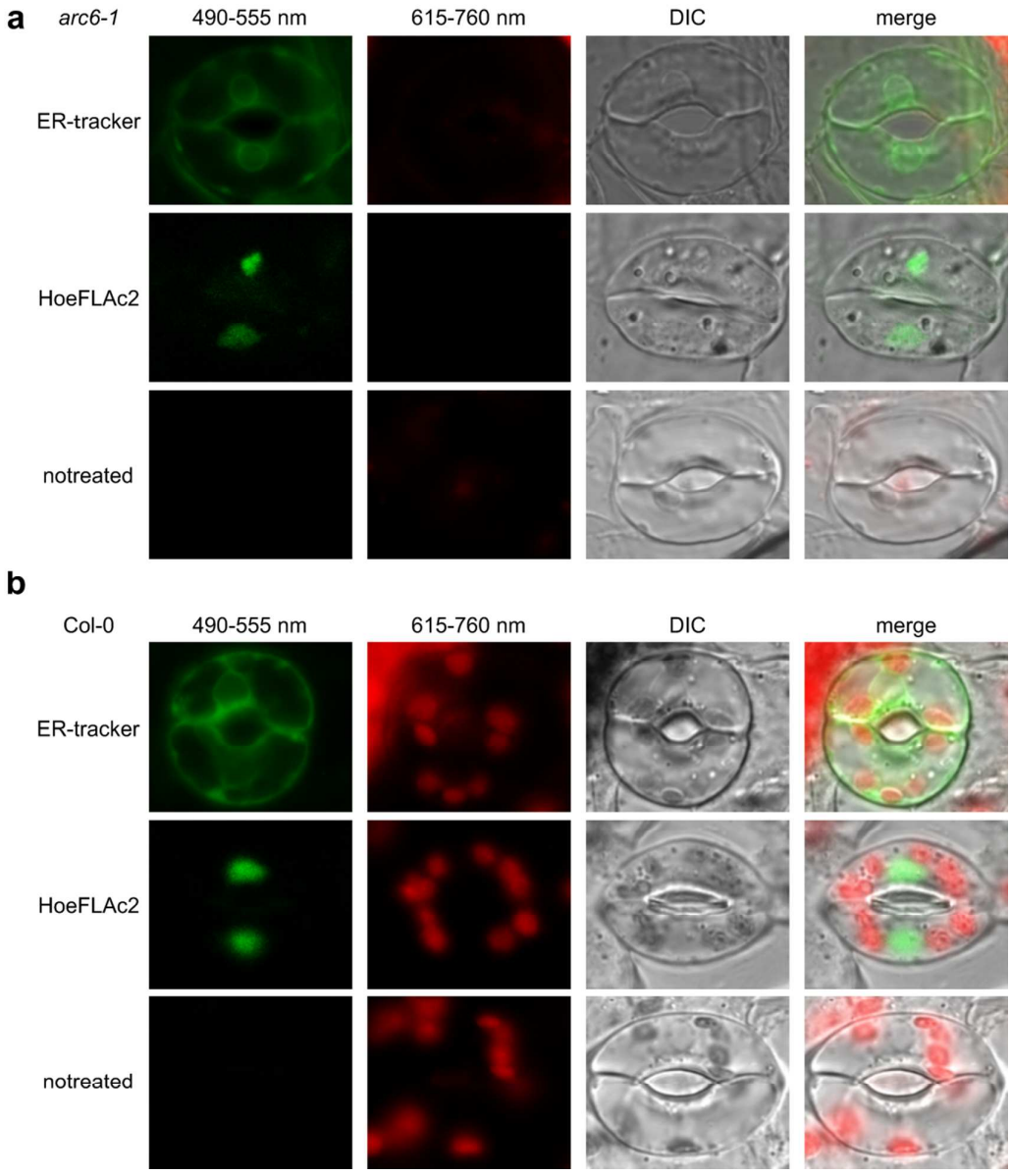

Figure S9. Fluorescent images of nucleus and ER in living guard cells of Col-0 and *arc6-1*. Fluorescence images and DIC images of *arc6-1* (**a**) and Col-0 (**b**). ER was stained by ER tracker, and nucleus was stained by $HoeFLAc_2$ [43]. Excitation wavelength was fixed at 488 nm, and images detected at 490-555 nm (left, green), at 610-735 nm (second left, red), DIC images (second right), merged images (right) were shown.

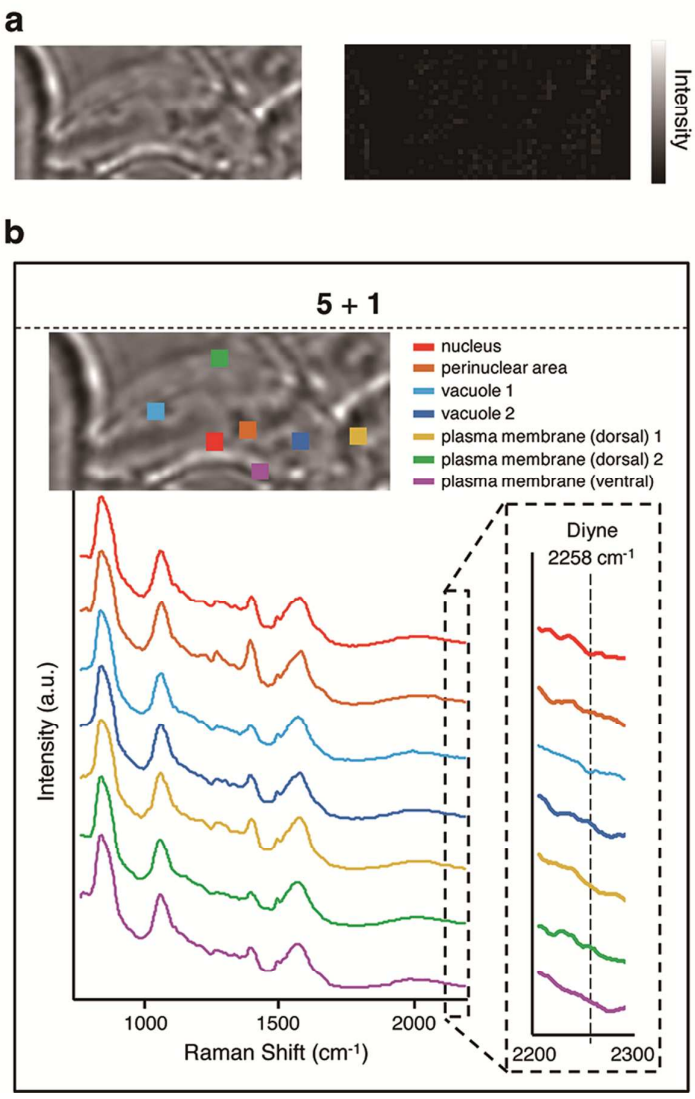

Figure S10. **Competitive inhibition of 5 with 1 in Raman Imaging**.

(**a**) Raman imaging in living guard cells of *A. thaliana arc6-1* after three hours of co-treatment with **1** (100 μM) and **5** (100 μM). Diyne Raman signal of **5** was not detected. The light intensity at the sample plane was calculated as 6.0 mW/μm^2 from the ratio of the measured laser power between the sample position and the illumination line. Exposure time for each line was 120 s. Spectra were vertically offset for ease viewing. (**b**) Raman spectra of each organelle region (1.2 μm × 1.1 μm: 3 × 3 = 9 pixels) of (**a**).

Scheme S1. Synthesis of **5**

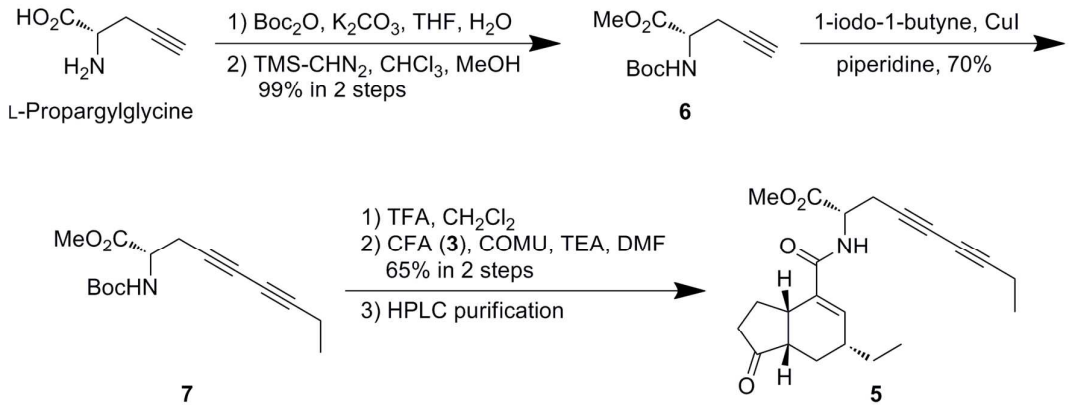

Table S1. Summary of the microarray analysis.

The ratios of inducible or suppressed genes treated with **1**, *ent***1** or **3**-*ent***4**, compared to mock treatment, are presented (**1**/mock, *ent***1**/mock, **3**-*ent***4**/mock).

Inducible genes both in **1**/mock and **3**-*ent***4**/mock

Accession No.	UniGeneID	GeneSymbol	**1**/mock	*ent***1**/mock	**3**-*ent***4**/mock
NM_114356	At.36095	*AT3G44870*	**205.8**	1.4	**11.3**
NM_114355	At.10101	*FAMT*	**135.2**	1.4	**8.9**
NM_102753	At.40613	*JAZ8*	**100.3**	-1.2	**11.6**
NM_001124015	At.74131	*AT1G53903*	**81.9**	1.5	**14.2**
NM_121325	At.26324	*JAZ10*	**81.5**	1.2	**6.4**
NM_203046	At.26324	*JAZ10*	**72.8**	-1.1	**6.1**
NM_106314	At.51311	*AT1G76640*	**68.2**	1.6	**8.9**
NM_001085035	At.28382	*MAPKKK21*	**62.7**	-2.6	**4.5**
NM_118304	At.32596	*MSRB8*	**59.2**	-1.4	**3.6**
NM_123658	At.55327	*AT5G42930*	**35.2**	1.6	**3.4**
NM_106579	At.34141	*MC7*	**33.5**	1.9	**2.6**
NM_125740	At.28998	*CYP94B1*	**33.0**	1.1	**3.9**
NM_129014	At.37783	*JAZ7*	**27.8**	1.2	**9.0**
NM_111830	At.49602	*AT3G09950*	**24.8**	1.1	**2.1**
NM_124611	At.29623	*CYP96A4*	**20.8**	1.3	**4.4**
NM_102616	At.11829	*GRX480*	**20.4**	1.0	**9.7**
NM_119606	At.48936	*RRTF1*	**20.3**	-1.6	**4.0**
NM_101599	At.27828	*JAZ5*	**20.2**	-1.2	**3.3**
NM_128328	At.13273	*CYP94C1*	**17.7**	1.4	**9.2**
NM_127138	At.13860	*AT2G15760*	**15.4**	1.7	**2.6**
NM_118303	At.25145	*MSRB7*	**15.2**	1.2	**2.5**
NM_001084589	At.75339	*AT2G44578*	**15.2**	1.4	**3.1**
NM_128498	At.12687	*GSTU6*	**15.0**	1.5	**2.3**
NM_124095	At.29907	*NUDT8*	**14.7**	1.2	**8.1**
NM_101580	At.10364	*GSTU26*	**14.6**	1.3	**2.0**
NM_121755	At.31541	*RGL3*	**14.2**	1.8	**2.7**
NM_104167	At.28621	*NAC019*	**14.1**	-2.0	**4.9**
NM_126108	At.49431	*MAPKKK19*	**14.1**	1.2	**5.9**
NM_001125571	At.48901	*AT4G24350*	**14.0**	1.4	**2.5**
NM_119946	At.31223	*AT4G37850*	**13.9**	1.6	**2.0**

BX813389	At.28621	*NAC019*	**13.9**	-1.5	**5.3**
NM_001036150	At.71985	*AT1G64195*	**13.6**	1.4	**2.3**
NM_121915	At.65529	*AT5G19100*	**13.1**	1.2	**2.6**
NM_129433	At.11759	*ANNAT3*	**12.9**	1.1	**2.7**
NM_001085002	At.44068	*AT4G29930*	**12.9**	1.1	**2.9**
NM_125071	At.49801	*AT5G56880*	**12.7**	-1.2	**2.2**
NM_121272	At.65507	*AT5G12340*	**12.7**	1.6	**5.5**
NM_101823	At.19779	*CLH1*	**12.3**	1.2	**2.1**
NM_114888	At.53871	*AT3G50280*	**12.1**	1.3	**2.5**
NM_112418	At.20460	*NAC3*	**11.2**	1.3	**7.7**
NM_115220	At.49399	*AT3G53600*	**10.9**	1.8	**5.1**
NM_120770	At.20009	*PGIP2*	**10.6**	1.1	**2.7**
NM_129837	At.36972	*AT2G42760*	**10.0**	1.6	**2.1**
NM_129432	At.20551	*ANNAT4*	**9.8**	-1.1	**2.5**
NM_106153	At.19896	*JAZ2*	**9.7**	1.4	**3.5**
NM_202133	At.22658	*JAZ1*	**9.2**	1.8	**5.0**
NM_117855	At.23185	*ERF-1*	**8.5**	1.9	**4.4**
AK221732	At.73177	*AT2G43540*	**8.5**	1.4	**3.7**
NM_125136	At.7483	*XTH25*	**8.5**	-1.7	**3.0**
AI995133	At.22648	*MYC2*	**8.3**	1.4	**3.1**
NM_125255	At.29268	*AT5G58680*	**7.7**	-1.1	**2.9**
NM_001035928	At.700	*ESL1*	**7.6**	1.1	**2.2**
CD530941	At.67560	*MSRB7*	**7.6**	1.2	**2.7**
NM_102998	At.22648	*MYC2*	**7.3**	1.5	**2.9**
NM_120642	At.8725	*AT5G05600*	**7.2**	1.2	**2.8**
NM_124093	At.19731	*ERF2*	**7.1**	1.7	**4.9**
NM_115837	At.54008	*AT3G59750*	**7.0**	1.6	**6.4**
NM_179700	At.43434	*NAI1*	**6.7**	1.2	**2.6**
NM_101603	At.20467	*LOX3*	**6.7**	1.1	**2.5**
NM_202143	At.15241	*OPCL1*	**6.5**	1.1	**2.7**
NM_106329	At.28236	*AT1G76790*	**6.5**	-1.0	**2.3**
NM_101507	At.11316	*CYP79F1*	**6.3**	1.3	**2.2**
NM_202111	At.11316	*CYP79F1*	**6.2**	1.3	**2.0**
NM_179009	At.47204	*RAP2.9*	**6.2**	1.2	**2.6**
NM_001084415	At.1135	*OPR3*	**6.1**	1.0	**2.3**
NM_128290	At.13633	*AT2G27310*	**5.7**	1.4	**2.7**

NM_124454	At.29715	*AT5G50760*	**5.6**	1.9	**2.2**
NM_106732	At.28188	*WRKY40*	**5.6**	-1.0	**2.2**
NM_105738	At.23705	*JAZ9*	**5.6**	1.3	**2.4**
NM_124172	At.29871	*AT5G47980*	**5.5**	1.6	**3.1**
NM_129313	At.37407	*AT2G37580*	**5.1**	1.2	**3.6**
NM_105604	At.24346	*CM3*	**5.0**	1.4	**2.1**
NM_105657	At.43696	*AT1G69890*	**4.9**	-1.2	**6.0**
NM_106569	At.10915	*MYB63*	**4.7**	1.5	**3.5**
NM_119904	At.22792	*CYP81F4*	**4.3**	1.1	**2.5**
DQ108691	At.8519	*PGIP1*	**4.3**	1.4	**2.5**
NM_129917	At.48587	*AT2G43550*	**4.2**	-1.1	**2.4**
DR381439	At.68141	*ERF-1*	**4.2**	1.3	**2.6**
NM_117550	At.23929	*APS3*	**4.2**	1.3	**3.1**
NM_128952	At.53026	*AT2G34010*	**4.2**	1.7	**2.4**
NM_202070	At.42241	*RBOHB*	**3.9**	1.2	**2.5**
NM_201808	At.64947	*AT2G26695*	**3.9**	1.7	**3.0**
NM_113475	At.26518	*AOC1*	**3.8**	1.2	**2.1**
NM_113476	At.6411	*AOC2*	**3.7**	1.4	**2.8**
NM_121892	At.54911	*AT5G18870*	**3.6**	1.6	**2.0**
NM_101427	At.28674	*IAA5*	**3.5**	1.3	**2.2**
BX814993	At.15581	*AT1G03440*	**3.4**	1.2	**2.3**
NM_001203302	At.285	*ASA1*	**3.3**	1.0	**2.0**
NM_203005	At.48988	*PAI2*	**3.3**	1.6	**2.2**
NM_148158	At.45475	*FLS4*	**3.2**	1.7	**3.3**
NM_119813	At.43740	*AT4G36500*	**3.1**	1.5	**2.3**
NM_127881	At.23258	*GH3.3*	**3.1**	1.3	**2.5**
BX820064	At.67889	*AT1G20520*	**3.0**	-1.1	**2.7**
NM_102256	At.10514	*UGT74B1*	**2.9**	1.4	**2.3**
NM_119047	At.3405	*AT4G29030*	**2.7**	1.8	**2.1**
NM_105366	At.35712	*PDR11*	**2.6**	1.1	**2.4**
NM_106309	At.19392	*AT1G76590*	**2.6**	1.2	**2.8**
NM_119299	At.24671	*CYP83B1*	**2.6**	1.2	**2.2**
NM_113478	At.37325	*AT3G25790*	**2.5**	2.0	**2.1**
NM_129921	At.24529	*AT2G43590*	**2.4**	1.1	**2.2**
NM_112507	At.1206	*AHP4*	**2.3**	1.3	**2.2**
NM_103224	At.39607	*MLP165*	**2.3**	1.3	**2.0**

NM_118903	At.32081	*AT4G27654*	**2.3**	-1.3	**2.8**
NM_104106	At.49487	*AT1G52270*	**2.3**	1.8	**4.3**
NM_115025	At.35368	*AT3G51660*	**2.2**	1.1	**2.0**
NM_120162	At.23161	*DHS1*	**2.1**	-1.1	**2.2**
NM_129195	At.43047	*PDR6*	**2.1**	-1.0	**2.1**
NM_114886	At.1423	*CEJ1*	**2.0**	-1.1	**2.7**
NM_127708	At.27499	*XK-1*	**2.0**	1.4	**3.3**

Suppressed genes both in **1**/mock and **3**-*ent***4**/mock

Accession No.	UniGeneID	GeneSymbol	**1**/mock	*ent***1**/mock	**3**-*ent***4**/mock
NM_128001	At.39164	*AT2G24400*	**-5.4**	-1.2	**-2.6**
NM_105562	At.26571	*bZIP*	**-3.7**	-1.2	**-2.6**
NM_122241	At.71067	*AT5G23350*	**-3.7**	-1.2	**-2.2**
NM_101897	At.69772	*AT1G20470*	**-3.3**	-1.8	**-4.1**
NM_119296	At.65443	*AT4G31470*	**-3.2**	1.3	**-2.1**
NM_123196	At.30414	*AT5G38350*	**-3.2**	-1.5	**-2.2**
NM_115373	At.35048	*EXO70H1*	**-3.1**	-1.1	**-2.1**
NM_105031	At.50800	*AT1G63530*	**-3.0**	-1.8	**-2.4**
NM_115310	At.53931	*AT3G54530*	**-2.9**	1.4	**-2.0**
NM_120233	At.49414	*LECRKA4.2*	**-2.7**	1.3	**-4.0**
NM_001123738	At.49840	*MPK11*	**-2.6**	1.3	**-3.2**
NM_148384	At.25207	*AT4G29905*	**-2.6**	-1.4	**-2.1**
NM_125015	At.29394	*EXPA14*	**-2.6**	-1.1	**-2.4**
NM_102442	At.51777	*AT1G26790*	**-2.5**	-1.3	**-14.1**
NM_113085	At.37979	*AT3G21890*	**-2.5**	-1.6	**-6.6**
NM_123329	At.19755	*AT5G39670*	**-2.5**	-1.7	**-2.8**
NM_113102	At.6152	*AT3G22060*	**-2.4**	1.3	**-2.0**
NM_114694	At.50254	*AT3G48240*	**-2.4**	-1.4	**-2.6**
NM_120232	At.28701	*LECRKA4.1*	**-2.4**	-1.9	**-2.2**
NM_001085091	At.72152	*IDL3*	**-2.4**	-1.6	**-2.9**
NM_122316	At.9177	*WRKY30*	**-2.4**	1.2	**-2.4**
NM_106211	At.34755	*AT1G75590*	**-2.4**	1.2	**-2.2**
NM_101756	At.41768	*AT1G18990*	**-2.4**	-1.9	**-2.0**
Z35201	At.71158	*AT1G80000*	**-2.3**	-1.8	**-2.4**
NM_123433	At.55282	*AT5G40680*	**-2.3**	-1.5	**-2.1**
NM_001085043	At.48962	*AT4G38560*	**-2.3**	-1.3	**-2.1**

NM_125360	At.55626	*AT5G59680*	**-2.3**	1.5	**-2.6**
NM_001126029	At.28918	*AT5G65140*	**-2.3**	-2.0	**-2.2**
NM_104866	At.66073	*AT1G61840*	**-2.2**	-1.3	**-2.1**
NM_103127	At.51926	*AT1G34050*	**-2.2**	-1.4	**-2.7**
NM_124803	At.9168	*MYB49*	**-2.2**	1.0	**-2.4**
NM_001125961	At.49174	*AT5G54130*	**-2.2**	-1.9	**-3.8**
NM_001123865	At.50783	*AT1G23110*	**-2.2**	1.1	**-2.0**
NM_179969	At.50123	*AT2G38823*	**-2.2**	1.1	**-2.0**
NM_001125881	At.69128	*AT5G41761*	**-2.2**	-1.9	**-2.0**
NM_122435	At.30922	*AT5G25260*	**-2.2**	-1.8	**-2.2**
NM_116474	At.34304	*AT4G02410*	**-2.2**	-1.2	**-2.2**
NM_111779	At.53235	*AT3G09450*	**-2.1**	-1.4	**-9.4**
NM_124134	At.29885	*AT5G47610*	**-2.1**	-1.5	**-2.2**
NM_113088	At.48689	*AT3G21920*	**-2.1**	1.2	**-2.2**
NM_111928	At.27986	*AT3G10910*	**-2.1**	1.2	**-2.8**
NM_128058	At.28320	*WRKY60*	**-2.1**	-1.6	**-2.1**
NM_117436	At.33355	*AT4G13620*	**-2.0**	1.1	**-2.1**
NM_113777	At.53543	*AT3G28570*	**-2.0**	1.5	**-2.1**
NM_117199	At.3654	*ACS6*	**-2.0**	-1.2	**-3.0**
NM_128762	At.38127	*AT2G32020*	**-2.0**	1.3	**-2.3**

Table S2 Sequences of all primers used for quantitative PCR

Allene oxide synthase	5’ CTCCGTTAATTTCTCGTC 3’
(*AOS*: AT5G42650)	3’ GCAGCAACAGATTATACAAC 5’
Vegetative Storage Protein 2	5’ AGATCAATGGGCTGATTTGG 3’
(*VSP2*: AT5G24770)	3’ GTGTATACAAGGGGACAATGCG 5’
Tubulin-alpha 5	5’ GGTGAGTATGATGTTGAAGA 3’
(*TUA*: AT5G19780)	3’ AGAGATTTCCAAGAGTCGT 5’

Table S3 Sequences of all primers used for Y2H

Jasmonate ZIM domain protein 9	5’ CACCATGGAAAGAGATTTTCTGG 3’
(*JAZ9*: AT1G70700)	3’ TGAGAAGATGAAGAGGATGTATT 5’
Coronatine Insensitive 1	5’ CACCATGGAGGATCCTGATATC 3’
(*COI1*: AT2G39940)	3’ TCAGGACTTCCTCGGTTATACT 5’

SI Materials & Methods

Microarray analysis

Total RNA was extracted from roots from 7-day-old seedlings using RNeasy Plant Mini Kit (QIAGEN, Germany). cDNAs were synthesized using 1.0 μg of total RNA and labeled with one color (Cy3) using a Quick Amp labeling kit (Agilent Technologies, USA), followed by fragmentation and hybridization to the *Arabidopsis* Oligo 44K DNA microarray (Ver. 4.0, Agilent Technologies, USA). Following fragmentation, 1.65 ug of cRNA were hybridized to the Agilent expression microarray according to the protocols provided by the manufacturer. All arrays were scanned with a microarray scanner (G2505B, Agilent Technologies, USA) and analyzed using Agilent Feature Extraction v11 (Agilent Technologies, USA). For microarray analysis, raw data were first filtered by a flag signal detected in all samples. Filtered raw data were processed using the Limma Bioconductor package (http://www.bioconductor.org/) in the R statistical environment (http://www.r-project.org/). After quantile normalization of data, miRNAs with twofold or greater differential expression were identified, with *P*-values of <0.05 being considered statistically significant.

Experimental Procedures for Raman Imaging and Spectroscopy

Experimental procedures used for **Figure S3**: Raman spectra obtained with a RAMAN-11 slit-scanning Raman microscope (Nanophoton, Japan) at 532 nm excitation. Samples were placed on a quartz substrate during the measurements. The laser output was focused into the sample by a 60X/1.2 NA UPLSAPO 60XW water immersion objective lens (Olympus Corp., Japan). The slit width of the spectrograph was 70 μm. The light intensity at the sample plane was calculated as 6.0 mW/μm^2 from the ratio of the measured laser power between the sample position and the area of the illumination line. The exposure time for each line was 120 s/line. Each sample solution was measured at 4 times.

Experimental procedures used for **Figure 4**: The abaxial leaf epidermis of 6- to 8-week-old Col-0 or *coi1-16s* was peeled and cut to about 2 mm^2. The peels were submerged in buffer (10 mM MES-KOH, pH 6.2, 50 mM KCl) at 22 °C for 3 h in the dark to close the stomata. After incubation for 3 h with 100 μM **5**/*ent***5** at 22 °C in the dark, peels were washed and then used for observation of bright-field images and Raman spectra obtained with a RAMAN-11 slit-scanning Raman microscope at 532 nm excitation. Samples were placed on a quartz substrate during the measurements. The laser output was focused into the sample by a 60X/1.2 NA UPLSAPO 60XW water immersion objective lens. The slit width of the spectrograph was 50 μm. The exposure time for each line was 120s/line. The laser intensity was calculated from the ratio of the measured laser power at the sample position and the illumination line. The light intensity at the sample plane was calculated as 6.2 mW/μm^2 (Col-0 with **5**), 6.1

mW/μm^2 (Col-0 with *ent***5**), 5.9 mW/μm^2 (*coi1-16s* with **5**), and 5.8 mW/μm^2 (*coi1-16s* with *ent***5**). Each Raman Spectra was Smoothed using a moving average method.

Experimental procedures used for **Figure S5**: The abaxial leaf epidermis of 6- to 8-week-old Col-0 or *arc6-1* was peeled and cut to about 2 mm^2. The peels were submerged in buffer (10 mM MES-KOH, pH 6.2, 50 mM KCl) at 22 °C for 3 h in the dark to close the stomata. After incubation for 3 h with 100 μM **5**/*ent***5** at 22 °C in the dark, peels were washed and then used for observation of bright-field images and Raman spectra obtained with a RAMAN-11 slit-scanning Raman microscope at 532 nm excitation. Samples were placed on a quartz substrate during the measurements. The laser output was focused into the sample by a 60X/1.2 NA UPLSAPO 60XW water immersion objective lens. The slit width of the spectrograph was 50 μm. The exposure time for each line was 120 s/line. The laser intensity was calculated from the ratio of the measured laser power at the sample position and the illumination line. The laser intensity of Col-0 was 6.2 mW/μm^2, *arc6-1* was 5.8 mW/μm^2. For Raman images in Fig. S3, the Raman spectral data set was un-processed Raman images were reconstructed using the peak intensity of average intensity of silent region (1985-2315 cm^{-1}). The final Col-0 images consist of 79 × 37 pixels and the final *arc6-1* images consists of 69 × 31 pixels.

Experimental procedures used for **Figure 5** and **Figures S7 and S8**: The abaxial leaf epidermis of 6- to 8-week-old *arc6-1* was peeled and cut to about 2 mm^2. The peels were submerged in buffer (10 mM MES-KOH, pH 6.2, 50 mM KCl) at 22 °C for 3 h in the dark to close the stomata. After incubation for 3 h with 100 μM **5**/*ent***5** at 22 °C in the dark, peels were washed and then used for observation of bright-field images and Raman spectra obtained with a RAMAN-11 slit-scanning Raman microscope at 532 nm excitation. Samples were placed on a quartz substrate during the measurements. The laser output was focused into the sample by a 60X/1.2 NA UPLSAPO 60XW water immersion objective lens. The slit width of the spectrograph was 50 μm. The exposure time for each line was 120-150 s/line. The laser intensity was calculated from the ratio of the measured laser power at the sample position and the illumination line. The light intensity at the sample plane was calculated as 6.0-6.2 mW/μm^2 (*arc6-1* with **5**), 6.2 mW/μm^2 (*arc6-1* with *ent***5**).

For Raman Spectra in **Figures S7 and S8**, each Raman Spectra was smoothed using a moving average method.

Experimental procedures used for **Figure S10**: The abaxial leaf epidermis of 6- to 8-week-old *arc6-1* was peeled and cut to about 2 mm^2. The peels were submerged in buffer (10 mM MES-KOH, pH 6.2, 50 mM KCl) at 22 °C for 3 h in the dark to close the stomata. After co-incubation for 3 h with 100 μM **1** and 100 μM **5** at 22 °C in the dark, peels were washed and then used for observation of bright-field images and Raman spectra obtained with a RAMAN-11 slit-scanning Raman microscope at 532 nm excitation. Samples were placed on a quartz

substrate during the measurements. The laser output was focused into the sample by a 60X/1.2 NA UPLSAPO 60XW water immersion objective lens. The slit width of the spectrograph was 70 μm. The exposure time for each line was 120 s/line. The laser intensity was calculated from the ratio of the measured laser power at the sample position and the illumination line. The light intensity at the sample plane was 6.0 mW/μm^2. Each Raman Spectra was smoothed using a moving average method.

For Raman images in **Figures 5 and S10**, the Raman spectral data set was further processed using the singular value decomposition (SVD) technique for noise reduction [44]. Then we used a narrow spectral region (1985-2315 cm^{-1}) in the calculation procedure for SVD to avoid artifacts in constructed images. A modified polyfit technique [45] was then used at each pixel to determine the autofluorescence baseline signal, which was subtracted from the original Raman spectrum. After SVD processing. Raman images were reconstructed using the peak intensity of diyne at 2,258 cm^{-1}. The final **5** images consist of 58 × 28 pixels and the final *ent***5** images consists of 78 × 34 pixels (**Figure 5**). The final **1** and **5** co-incubated images consist of 57 × 27 pixels (**Figure S10**).

.

Experimental Procedures for Fluorescence Imaging

Experimental procedures used for **Figure S5**: To examine nuclear and ER localization, the abaxial leaf epidermis of 6- to 8-week-old Col-0 or *arc6-1* was peeled and cut to about 2 mm^2. Light micrographs and fluorescent images were taken using an IX71 microscope (Olympus Corp., Japan) equipped with DP72 CCD camera (Olympus Corp., Japan) and WIB filter (Olympus Corp., Japan).

Experimental procedures used for **Figures 5** and **S9**: To examine nuclear and ER localization, the abaxial leaf epidermis of 6- to 8-week-old Col-0 or *arc6-1* was peeled and cut to about 2 mm^2. The peels were incubated with test compounds in buffer (10 mM MES-KOH, pH 6.2, 50 mM KCl) containing 0.5% DMSO at 22 °C in the dark a) for 90 min without compounds b) for 90 min with 5 μM of $HoeFLAc_2$ [43] and c) for 90 min with 5 μM ER-Tracker Green (Thermo Fisher Scientific, Inc., USA). Light micrographs and fluorescent images were taken using or an LSM-710 confocal microscope system (Carl Zeiss, Germany).

General Experimental Procedures for Chemical Synthesis

^{1}H NMR and ^{13}C NMR spectra in $CDCl_3$ were recorded on a JNM-ECS-400 NMR spectrometer (JEOL Inc., Japan). High-resolution electrospray ionization mass spectrometry was carried out on a micrOTOF II mass spectrometer (Bruker Daltonics Inc., Germany). Chemical reagents and solvents were purchased from Kanto Chemical Co. Ltd. (Japan), Wako

Pure Chemical Industries Co. Ltd. (Japan), and Nacalai Tesque, Inc. (Japan). All anhydrous solvents were dried by standard techniques and freshly distilled before use or purchased in anhydrous form. Flash chromatography was carried out using dry-packed Chromatorex PSQ 100B silica gel (Fuji Silysia Chemical Ltd., Japan). All reactions were carried out under air unless stated otherwise. FT/IR spectra were recorded on a JASCO FT/IR-4100 spectrometer (JASCO Inc., Japan). Optical rotation was measured by a JASCO DIP-1000 polarimeter. High performance liquid chromatography was carried out with a combination of a JASCO PU-2086 Plus pump and JASCO UV-2075 detector equipped with a Develosil RP-AQUEOUS ϕ20 × 250 mm column (Nomura Chemical, Co., Ltd., Japan). Freeze-drying was performed using a EYELA FDU-830 freeze dryer system (Tokyo Rikakikai Co., Ltd., Japan).

Experimental Procedures for Synthesis and compound data

Methyl (*S*)-2-((*tert*-butoxycarbonyl)amino)pent-4-ynoate (**6**)

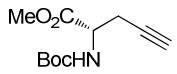

6

To a solution of L-propargylglycine [CAS No.23235-01-0] (113.1 mg, 1.00 mmol) in THF/DMF/H_2O (1/1/1, 12.0 mL) was added di-*tert*-butyl dicarbonate (250 μL, 1.09 mmol) and K_2CO_3 (139 mg, 1.00 mmol) at room temperature under argon atmosphere. After the reaction mixture was stirred for 2 h, the mixture was extracted by saturated aqueous $NaHCO_3$. (3 × 30 mL). The aqueous layer was mixed with 5% aqueous $KHSO_4$ (150 mL) and extracted with EtOAc (3 × 50 mL). The organic layer was dried over Ns_2SO_4, and filtered. After evaporation, the residue was dissolved in $CHCl_3$/MeOH (3/1, 8.0 mL) and mixed with 1.6 M trimethylsilyldiazomethane in *n*-hexane (2.0 mL) at room temperature under argon atmosphere. After the reaction was stirred for 10 min, the reaction was quenched by acetic acid and then the mixture was evaporated. The residue was purified by silica gel column chromatography (*n*-hexane/EtOAc = 15/1) to give **6** (225.3 mg, 0.991 mmol, 99%) as a colorless oil. ^{1}H NMR (400 MHz, $CDCl_3$) δ_H: 5.35 (d, J = 8.4, 1H), 4.48 (dt, J = 8.4, 4.8, 1H), 3.78 (s, 3H), 2.78–2.68 (m, 2H), 2.04 (t, J = 2.8, 1H), 1.46 (s, 9H); ^{13}C NMR (100 MHz, $CDCl_3$) δ_C: 171.1, 155.1, 80.2, 78.5, 71.6, 52.6, 51.9, 28.2(3C), 22.8; IR (film) cm^{-1}: 3294, 2978, 2958, 2123, 1750, 1713, 1506, 1439, 1358, 1064, 1025, 994; HRMS (ESI, positive) *m/z* $[M+Na]^+$ calcd. for $C_{11}H_{17}NO_4Na$: 250.1050, Found : 2501059; $[\alpha]_D^{21}$ +57.8° (c = 0.89, $CHCl_3$)

Methyl (*R*)-2-((*tert*-butoxycarbonyl)amino)pent-4-ynoate (*ent***6**)

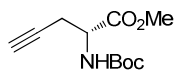

*ent***6**

*Ent***6** was prepared from D-propargylglycine [CAS No. 23235-03-2] according to the same

method as **6**. ^{1}H NMR (400 MHz, $CDCl_3$) δ_H: 5.35 (d, J = 8.4, 1H), 4.48 (dt, J = 8.4, 4.8, 1H), 3.78 (s, 3H), 2.78–2.68 (m, 2H), 2.04 (t, J = 2.8, 1H), 1.46 (s, 9H); ^{13}C NMR (100 MHz, $CDCl_3$) δ_C: 171.1, 155.1, 80.2, 78.5, 71.6, 52.6, 51.9, 28.3(3C), 22.8; IR (film) cm^{-1}: 3294, 2978, 2958, 2123, 1750, 1713, 1506, 1439, 1358, 1064, 1025, 994; HRMS (ESI, positive) *m/z* $[M+Na]^+$ calcd. for $C_{11}H_{17}NO_4Na$: 250.1050, Found : 250.1042; $[\alpha]_D^{21}$ –58.9° (c = 0.77, $CHCl_3$)

Methyl (*S*)-2-((*tert*-butoxycarbonyl)amino)nona-4,6-diynoate (**7**)

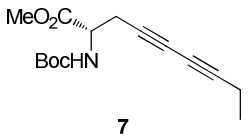

7

To a solution of **6** (132.1 mg, 0.581 mmol) in piperidine (2.5 mL) was added 1-butynyl iodide [CAS No.66794-29-4] (100 μL, 0.966 mmol) and copper (I) iodide (57 mg, 29.9 μmol) at 0 °C under argon atmosphere. After 4 h stirring, the reaction was quenched with 5 % aqueous $KHSO_4$ (30 mL). The reaction mixture was extracted with EtOAc (3 × 20 mL), and then the organic layer was dried over Na_2SO_4 and filtered. After evaporation, the residue was purified by silica gel column chromatography (*n*-hexane/EtOAc = 15/1) to give **7** (111.4 mg, 0.408 mmol, 70%) as a white solid. ^{1}H NMR (400 MHz, $CDCl_3$) δ_H: 5.33 (d, J = 8.4, 1H), 4.46 (dt, J = 8.4, 4.8, 1H), 3.78 (s, 3H), 2.86–2.75 (m, 2H), 2.26 (q, J = 7.2, 2H), 1.46 (s, 9H), 1.15 (t, J = 7.2, 3H); ^{13}C NMR (100 MHz, $CDCl_3$) δ_C: 170.9, 155.0, 80.2, 79.9, 71.0, 68.3, 64.2, 52.7, 52.0, 28.2(3C), 23.7, 13.2, 12.8.; IR (film) cm^{-1}: 3366, 2980, 2939, 2260, 1749, 1715, 1508, 1436, 1267, 1251, 1218, 1168, 1062, 778; HRMS (ESI, positive) *m/z* $[M+Na]^+$ calcd. for $C_{15}H_{21}NO_4Na$: 302.1363, Found : 302.1360;$[\alpha]_D^{21}$ +94.5° (c = 0.78, $CHCl_3$).

Methyl (*R*)-2-((*tert*-butoxycarbonyl)amino)nona-4,6-diynoate (*ent***7**)

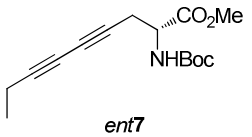

*ent***7**

*Ent***7** was prepared from *ent***6** according to the same method as **7**. ^{1}H NMR (400 MHz, $CDCl_3$) δ_H: 5.33 (d, J = 8.4, 1H), 4.46 (dt, J = 8.4, 4.8, 1H), 3.78 (s, 3H), 2.86–2.75 (m, 2H), 2.26 (q, J = 7.2, 2H), 1.46 (s, 9H), 1.15 (t, J = 7.2, 3H); ^{13}C NMR (100 MHz, $CDCl_3$) δ_C: 170.9, 155.0, 80.2, 79.9, 71.0, 68.3, 64.3, 52.7, 52.0, 28.3(3C), 23.7, 13.2, 12.8; IR (film) cm^{-1}: 3366, 2980, 2939, 2260, 1749, 1715, 1508, 1436, 1267, 1251, 1218, 1168, 1062, 778; HRMS (ESI, positive) *m/z* $[M+Na]^+$ calcd. for $C_{15}H_{21}NO_4Na$: 302.1363, Found : 302.1351; $[\alpha]_D^{21}$ –94.5° (c = 0.90 in $CHCl_3$)

Methyl (*S*)-2-((3a*S*,6*R*,7a*S*)-6-ethyl-1-oxo-2,3,3a,6,7,7a-hexahydro-1*H*-indene-4-carboxamido)nona-4,6-diynoate (**5**)

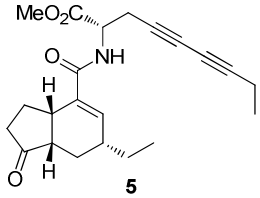

5

To a solution of **7** (6.6 mg, 23.6 μmol) in CH_2Cl_2 (0.8 mL) was added TFA (0.2 mL) at room temperature under argon atmosphere. After 30 min stirring, the reaction mixture was evaporated and the residue was dissolved in DMF (1.0 mL). To this solution, CFA (**3**) [22] (5.2 mg, 25.0 μmol), COMU (12.9 mg, 30.1 μmol) and TEA (7.26 mg, 71.7 μmol) were added at room temperature under argon atmosphere. After overnight stirring, the reaction was quenched by 5% aqueous $KHSO_4$ (5 mL), and then the mixture was extracted with EtOAc (10 mL). The organic layer was washed with 5% aqueous $KHSO_4$ (2 × 3 mL), saturated aqueous $NaHCO_3$ (2 × 3 mL), and brine (3 mL), and then dried over Na_2SO_4 and filtered. After evaporation, the residue was purified by silica gel column chromatography (*n*-hexane/EtOAc = 4/1) to give **5** (6.0 mg, 15.3 μmol, 65%). Moreover, the **5** (3.9 mg) was purified by HPLC (mobile phase: CH_3OH / H_2O = 60 / 40, flow rate: 8.0 mL/min) on Develosil RPAQUEOUS (ϕ20 × 250 mm, Nomura Chemicals Co. Ltd., Japan) to give **5** (3.6 mg, Rt = 71–75 min) as a colorless crystal. ^{1}H NMR (400 MHz, $CDCl_3$) δ_H: 6.59 (d, *J* = 7.6 Hz, 1H), 6.49 (s, 1H), 4.80 (dt, *J* = 7.6, 4.4 Hz, 1H), 3.93 (s, 3H), 3.17 (dt, *J* = 11.6, 6.8 Hz, 1H), 2.90 (dd, *J* = 17.2, 4.4 Hz, 2H), 2.52–2.12 (m, 7H), 1.90 (dt, *J* = 13.2, 4.8 Hz, 1H), 1.69–1.36 (m, 3H), 1.15 (t, *J* = 7.6 Hz, 3H), 1.08 (td, *J* = 13.2, 10.8 Hz, 1H), 1.01 (t, *J* = 7.6 Hz, 3H); ^{13}C NMR (100 MHz, $CDCl_3$) δ_C: 220.2, 170.9, 167.5, 139.1, 135.0, 80.1, 70.9, 68.6, 64.1, 53.0, 50.7, 46.5, 39.2, 37.4, 36.1, 28.0, 27.8, 26.0, 23.3, 13.2, 12.9, 11.3.; IR (film) cm^{-1}: 3335, 2961, 2939, 2879, 2858, 2260, 1741, 1654, 1624, 1521, 1457, 1437, 1350, 1317, 1262, 1219, 1148, 1069; HRMS (ESI, positive) *m/z* $[M+Na]^+$ calcd. for $C_{22}H_{27}NO_4Na$: 392.1832, Found : 392.1825; $[\alpha]_D^{21}$ +115° (c = 0.18 in $CHCl_3$).

Methyl (*R*)-2-((3a*R*,6*S*,7a*R*)-6-ethyl-1-oxo-2,3,3a,6,7,7a-hexahydro-1*H*-indene-4-carboxamido)nona-4,6-diynoate (*ent***5**)

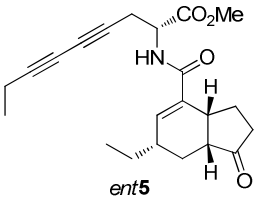

*ent***5**

*Ent***5** was prepared from *ent***7** with *ent***3** [22] according to the same method as **5**. ^{1}H NMR (400 MHz, $CDCl_3$) δ_H: 6.59 (d, *J* = 7.6 Hz, 1H), 6.49 (s, 1H), 4.80 (dt, *J* = 7.6, 4.4 Hz, 1H), 3.93 (s, 3H), 3.17 (dt, *J* = 11.6, 6.8 Hz, 1H), 2.90 (dd, *J* = 17.2, 4.4 Hz, 2H), 2.52–2.12 (m, 7H), 1.90 (dt, *J* = 13.2, 4.8 Hz, 1H), 1.69–1.36 (m, 3H), 1.15 (t, *J* = 7.6 Hz, 3H), 1.08 (td, *J* = 13.2, 10.8 Hz, 1H), 1.01 (t, *J* = 7.6 Hz, 3H); ^{13}C NMR (100 MHz, $CDCl_3$) δ_C: 220.2, 170.9, 167.5, 139.0, 135.0, 80.1, 70.9, 68.6, 64.1, 53.0, 50.7, 46.5, 39.2, 37.4, 36.1, 28.0, 27.8, 26.1, 23.3, 13.2, 12.9, 11.3; IR (film) cm^{-1}: 3317, 2960, 2939, 2877, 2857, 2260, 1741, 1655, 1624, 1522, 1457, 1436, 1349, 1317, 1274, 1218, 1148, 1068.; HRMS (ESI, positive) *m/z* $[M+Na]^+$ calcd. for $C_{22}H_{27}NO_4Na$: 392.1832, Found : 392.1824; $[\alpha]_D^{21}$ –116° (c = 0.20 in $CHCl_3$).

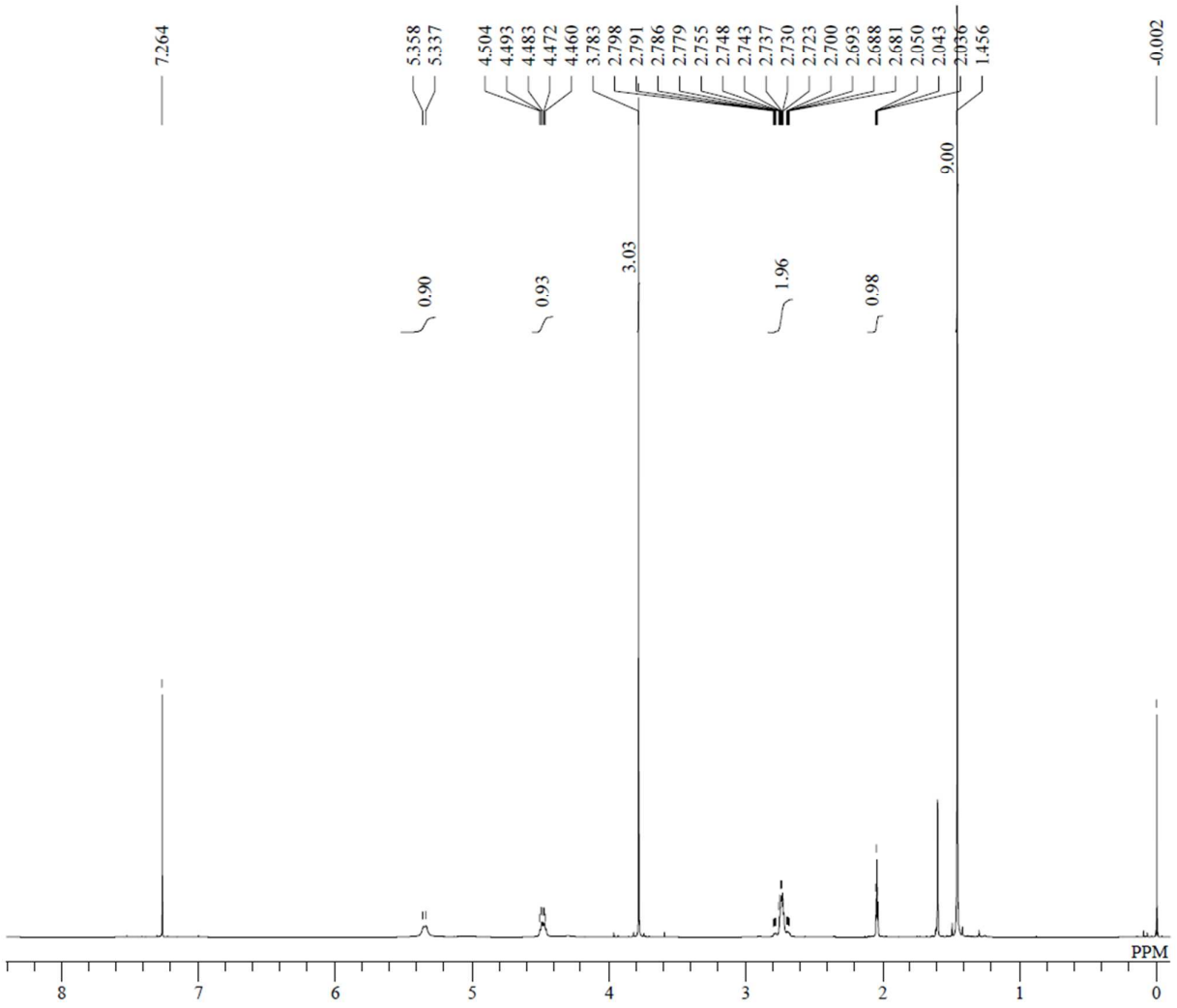

DFILE	(+)-7_1H.als
COMNT	single_pulse
DATIM	15-10-2015 19:49:53
OBNUC	1H
EXMOD	proton.jxp
OBFRQ	399.78 MHz
OBSET	4.19 KHz
OBFIN	7.29 Hz
POINT	13107
FREQU	6002.40 Hz
SCANS	16
ACQTM	2.1837 sec
PD	5.0000 sec
PW1	2.95 usec
IRNUC	1H
CTEMP	23.9 c
SLVNT	CDCL3
EXREF	7.26 ppm
BF	0.12 Hz
RGAIN	48

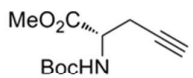

6

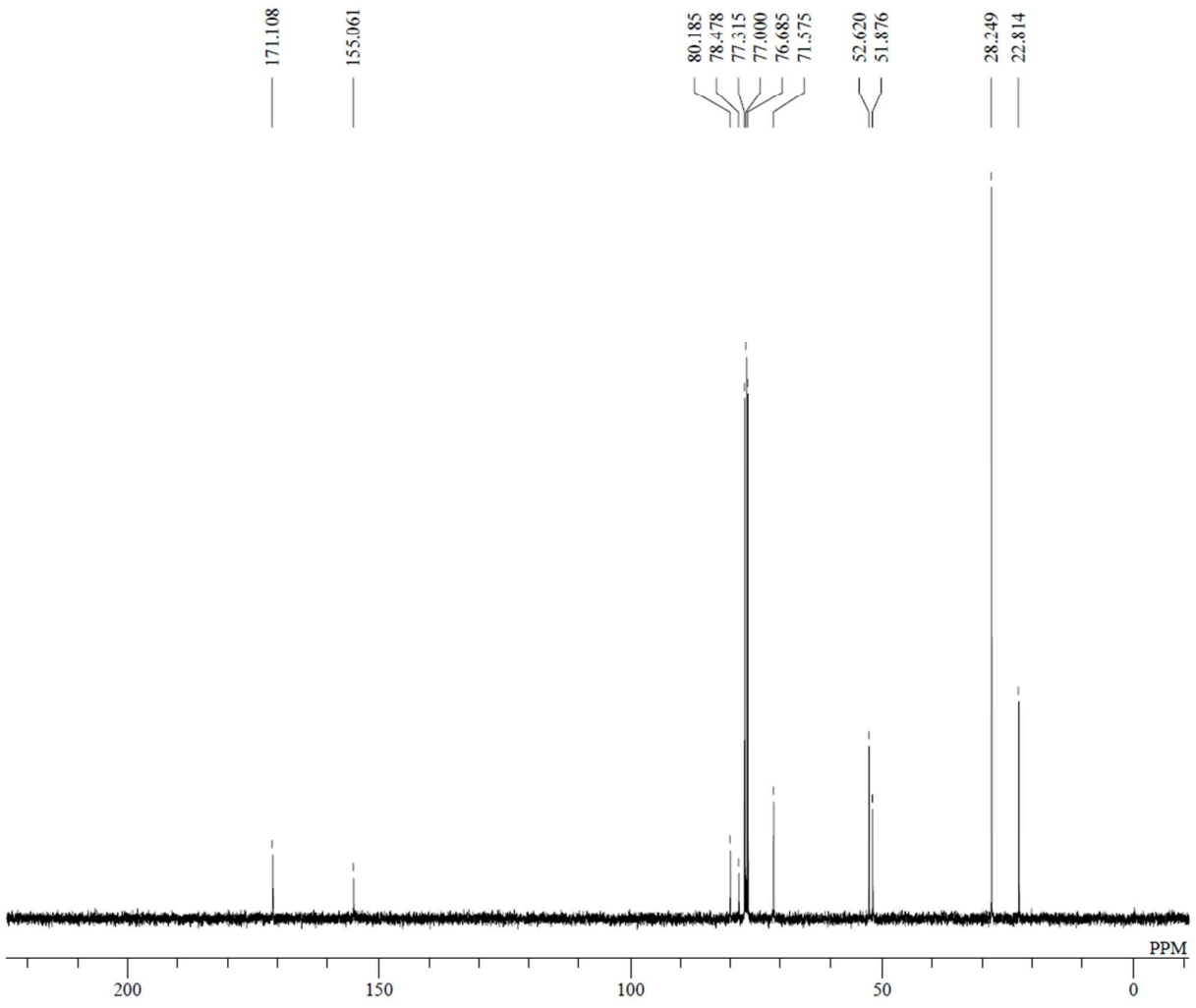

DFILE	(+)-7_13C.als
COMNT	single pulse decoupled
DATIM	04-06-2013 14:48:33
OBNUC	13C
EXMOD	carbon.jxp
OBFRQ	100.53 MHz
OBSET	5.35 KHz
OBFIN	5.86 Hz
POINT	26214
FREQU	25125.63 Hz
SCANS	512
ACQTM	1.0433 sec
PD	2.0000 sec
PW1	2.38 usec
IRNUC	1H
CTEMP	24.0 c
SLVNT	CDCL3
EXREF	77.00 ppm
BF	1.20 Hz
RGAIN	50

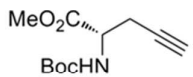

6

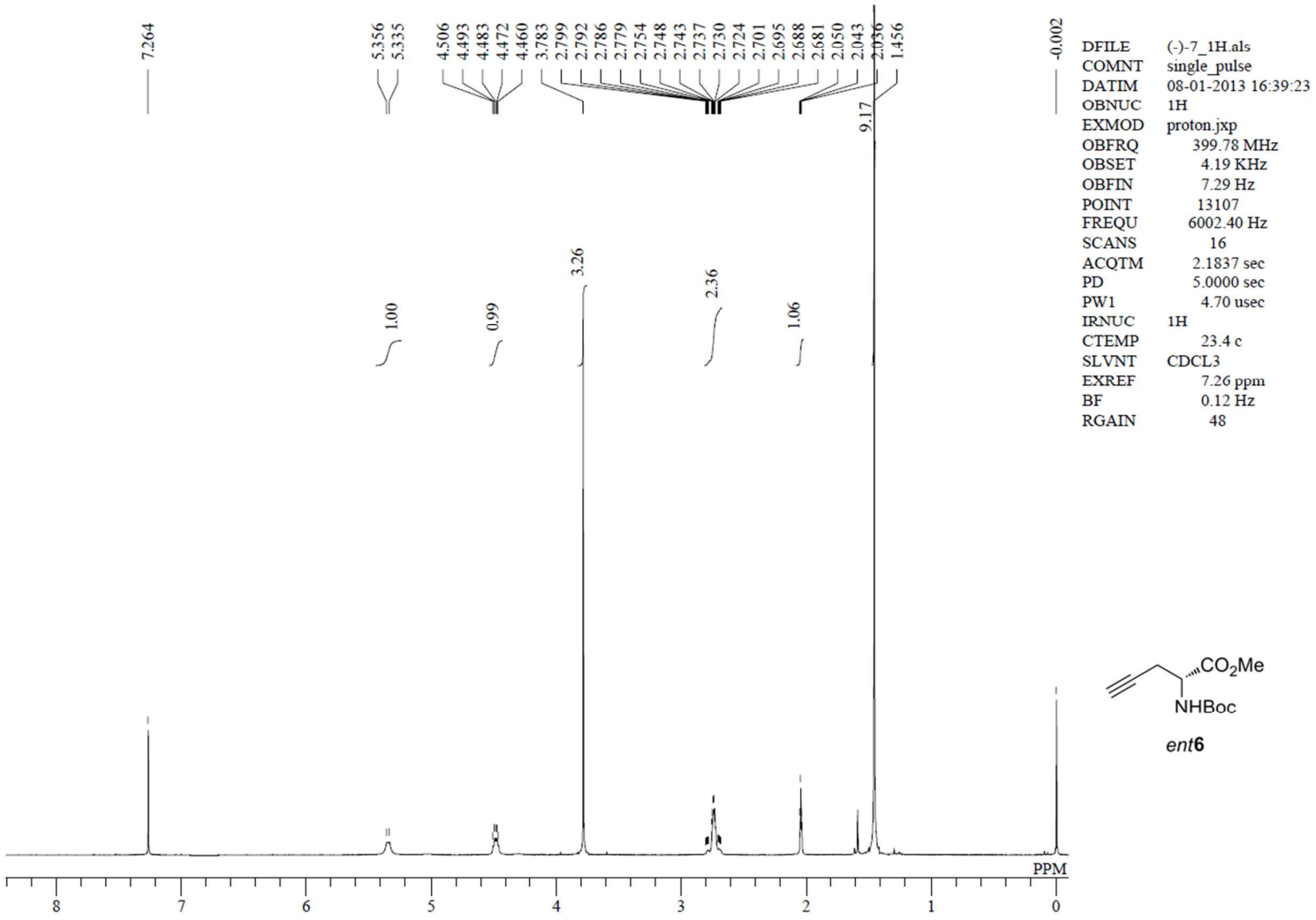

DFILE	(-)-7_1H.als
COMNT	single_pulse
DATIM	08-01-2013 16:39:23
OBNUC	1H
EXMOD	proton.jxp
OBFRQ	399.78 MHz
OBSET	4.19 KHz
OBFIN	7.29 Hz
POINT	13107
FREQU	6002.40 Hz
SCANS	16
ACQTM	2.1837 sec
PD	5.0000 sec
PW1	4.70 usec
IRNUC	1H
CTEMP	23.4 c
SLVNT	CDCL3
EXREF	7.26 ppm
BF	0.12 Hz
RGAIN	48

*ent***6**

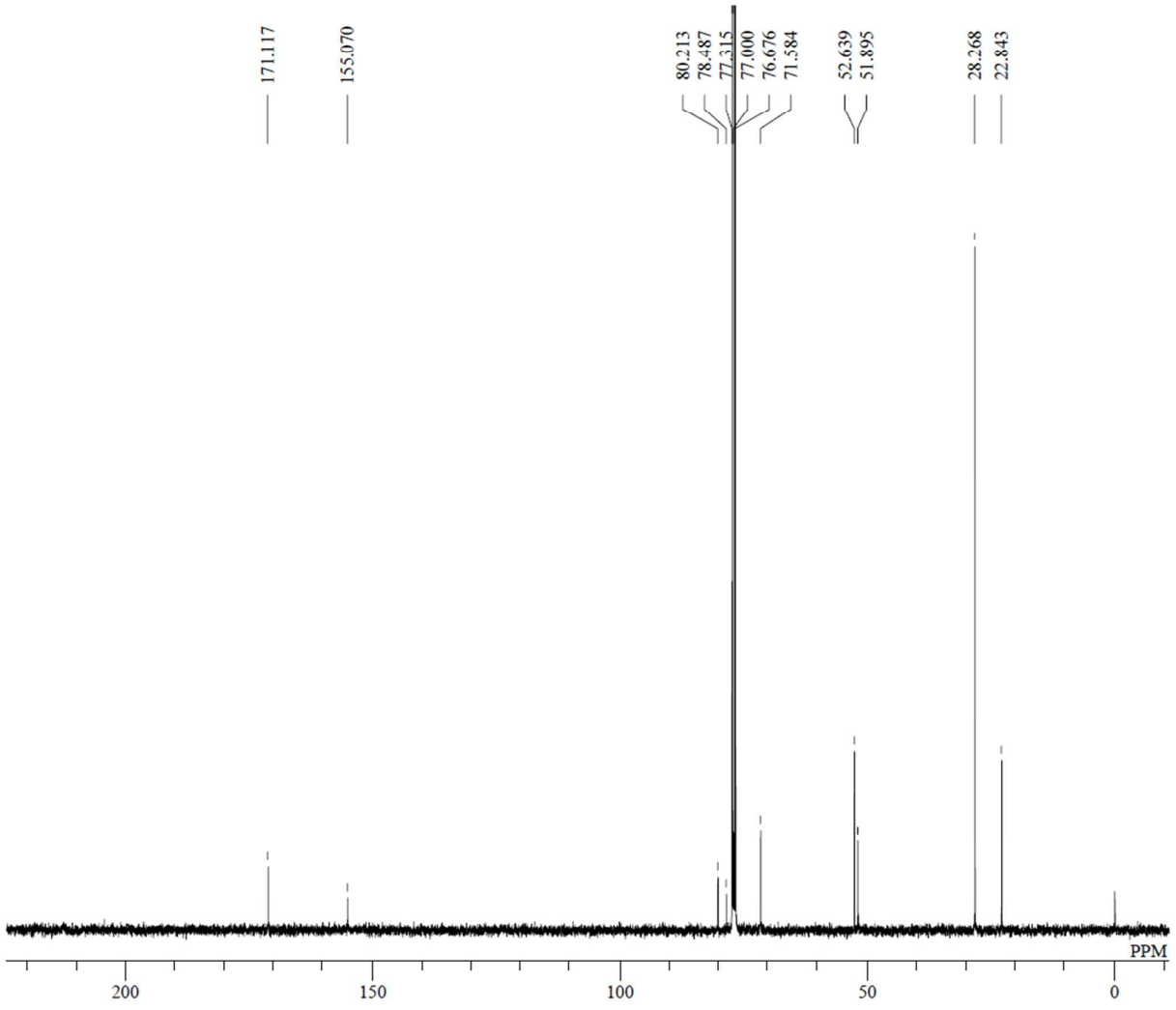

DFILE	(-)-7_13C.als
COMNT	single pulse decoupled
DATIM	16-10-2015 08:05:55
OBNUC	13C
EXMOD	carbon.jxp
OBFRQ	100.53 MHz
OBSET	5.35 KHz
OBFIN	5.86 Hz
POINT	26214
FREQU	25125.63 Hz
SCANS	2048
ACQTM	1.0433 sec
PD	2.0000 sec
PW1	3.37 usec
IRNUC	1H
CTEMP	24.3 c
SLVNT	CDCL3
EXREF	77.00 ppm
BF	1.20 Hz
RGAIN	60

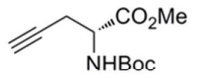

*ent***6**

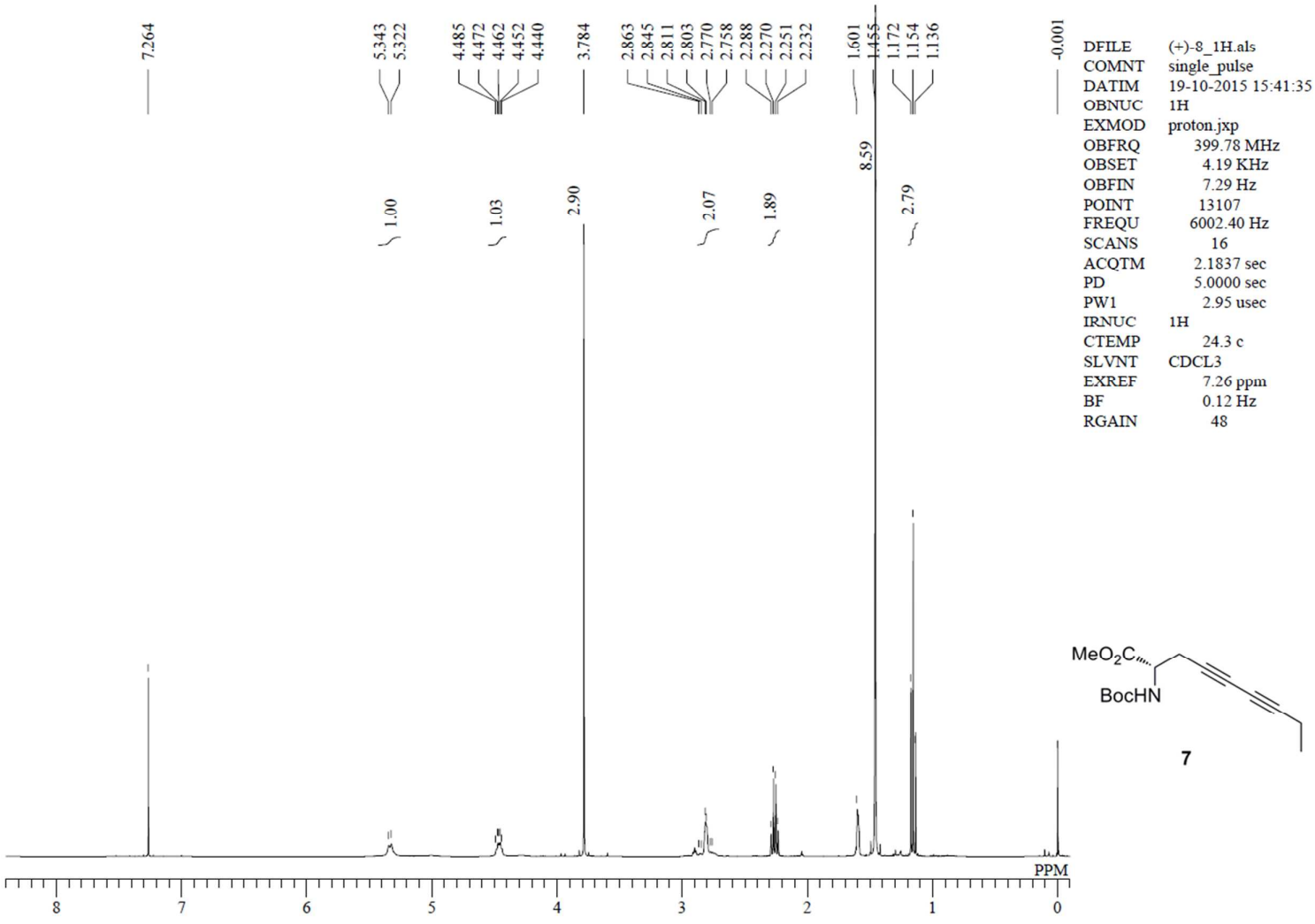

DFILE	(+)-8_1H.als
COMNT	single_pulse
DATIM	19-10-2015 15:41:35
OBNUC	1H
EXMOD	proton.jxp
OBFRQ	399.78 MHz
OBSET	4.19 KHz
OBFIN	7.29 Hz
POINT	13107
FREQU	6002.40 Hz
SCANS	16
ACQTM	2.1837 sec
PD	5.0000 sec
PW1	2.95 usec
IRNUC	1H
CTEMP	24.3 c
SLVNT	CDCL3
EXREF	7.26 ppm
BF	0.12 Hz
RGAIN	48

7

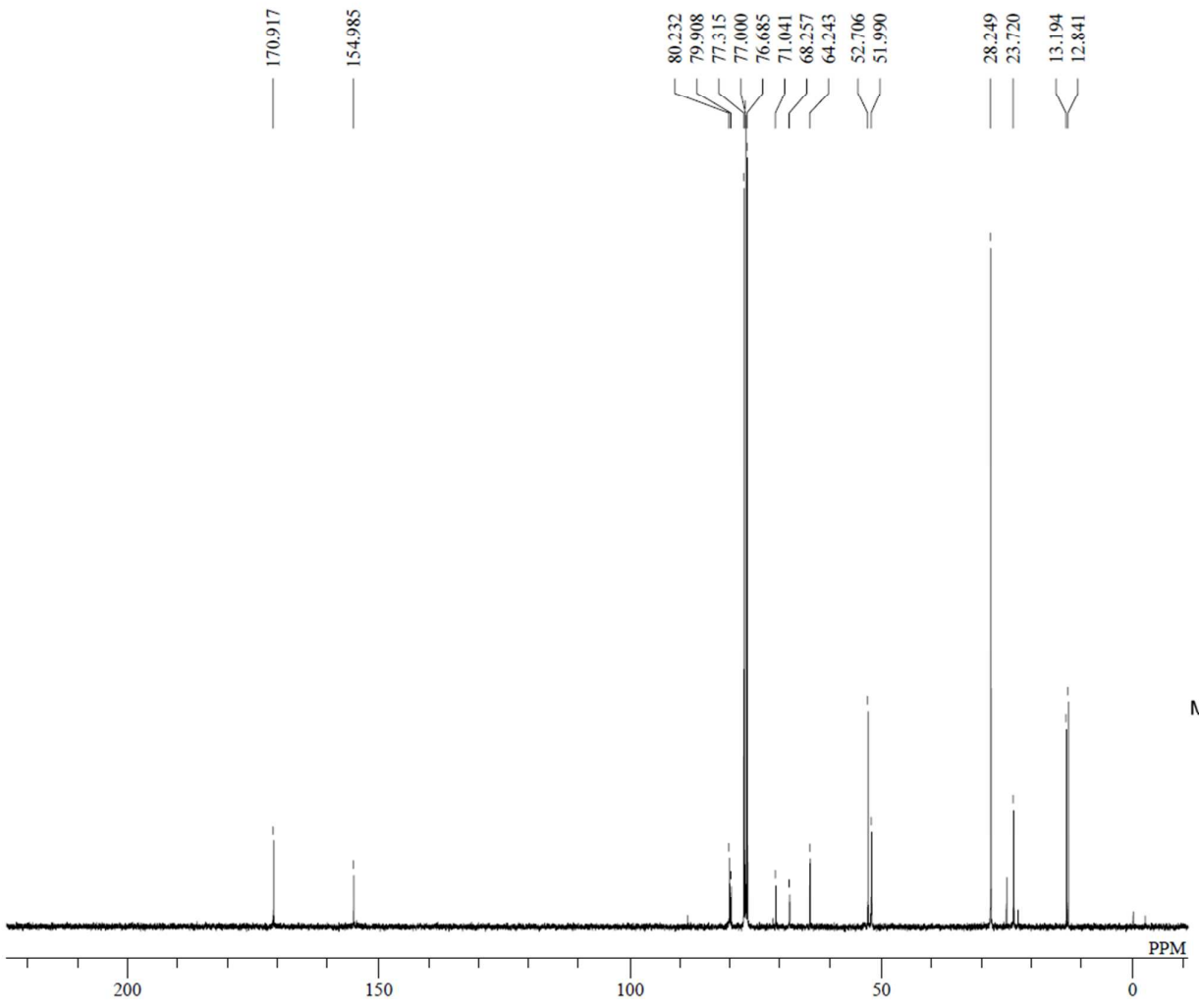

DFILE	(+)-8_13C.als
COMNT	single pulse decoupled
DATIM	17-10-2015 07:30:51
OBNUC	13C
EXMOD	carbon.jxp
OBFRQ	100.53 MHz
OBSET	5.35 KHz
OBFIN	5.86 Hz
POINT	26214
FREQU	25125.63 Hz
SCANS	2048
ACQTM	1.0433 sec
PD	2.0000 sec
PW1	3.37 usec
IRNUC	1H
CTEMP	23.9 c
SLVNT	CDCL3
EXREF	77.00 ppm
BF	1.20 Hz
RGAIN	50

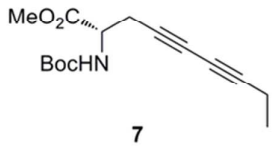

7

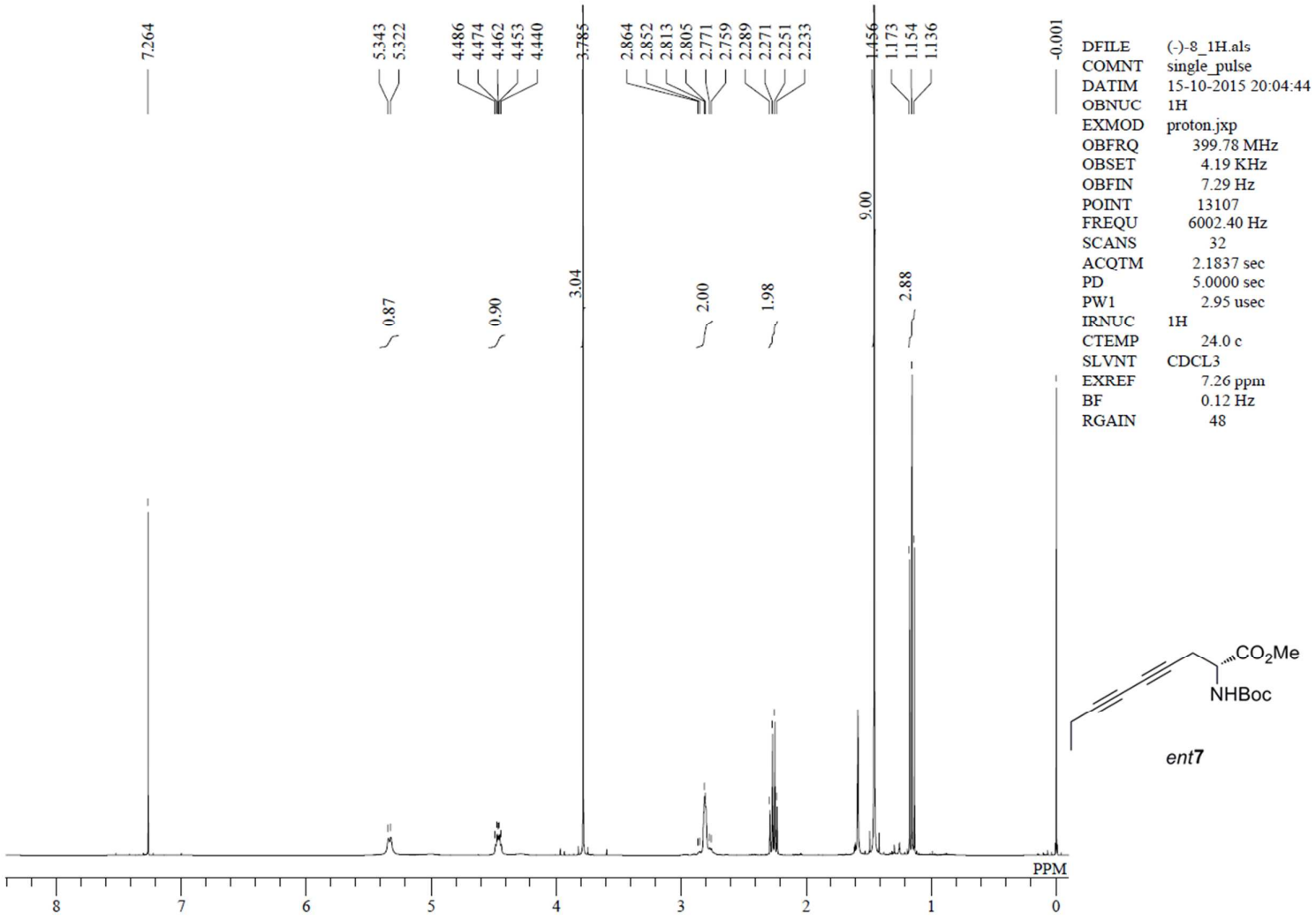
7.264
5.343
5.322
4.486
4.474
4.462
4.453
4.440
3.785
2.864
2.852
2.813
2.805
2.771
2.759
2.289
2.271
2.251
2.233
1.456
1.173
1.154
1.136
-0.001
0.87
0.90
3.04
2.00
1.98
9.00
2.88
PPM
8
7
6
5
4
3
2
1
0
DFILE (-)-8_1H.als
COMNT single_pulse
DATIM 15-10-2015 20:04:44
OBNUC 1H
EXMOD proton.jxp
OBFRQ 399.78 MHz
OBSET 4.19 KHz
OBFIN 7.29 Hz
POINT 13107
FREQU 6002.40 Hz
SCANS 32
ACQTM 2.1837 sec
PD 5.0000 sec
PW1 2.95 usec
IRNUC 1H
CTEMP 24.0 c
SLVNT CDCL3
EXREF 7.26 ppm
BF 0.12 Hz
RGAIN 48
CO2Me
NHBoc
ent7

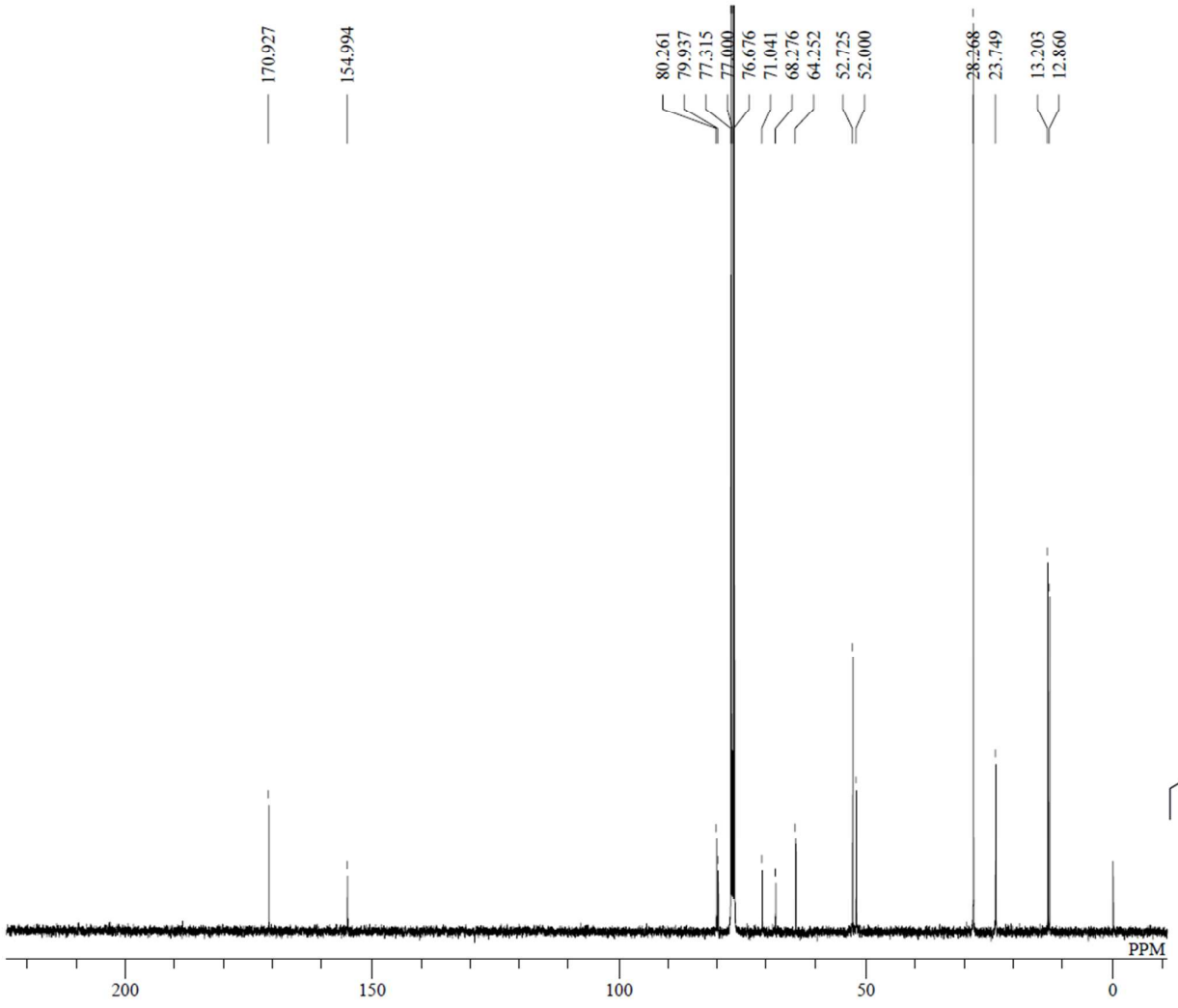

DFILE	(-)-8_13C.als
COMNT	single pulse decoupled
DATIM	16-10-2015 00:29:40
OBNUC	13C
EXMOD	carbon.jxp
OBFRQ	100.53 MHz
OBSET	5.35 KHz
OBFIN	5.86 Hz
POINT	26214
FREQU	25125.63 Hz
SCANS	8192
ACQTM	1.0433 sec
PD	2.0000 sec
PW1	3.37 usec
IRNUC	1H
CTEMP	24.2 c
SLVNT	CDCL3
EXREF	77.00 ppm
BF	1.20 Hz
RGAIN	60

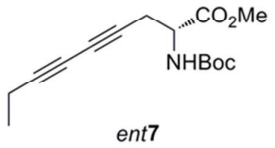

*ent***7**

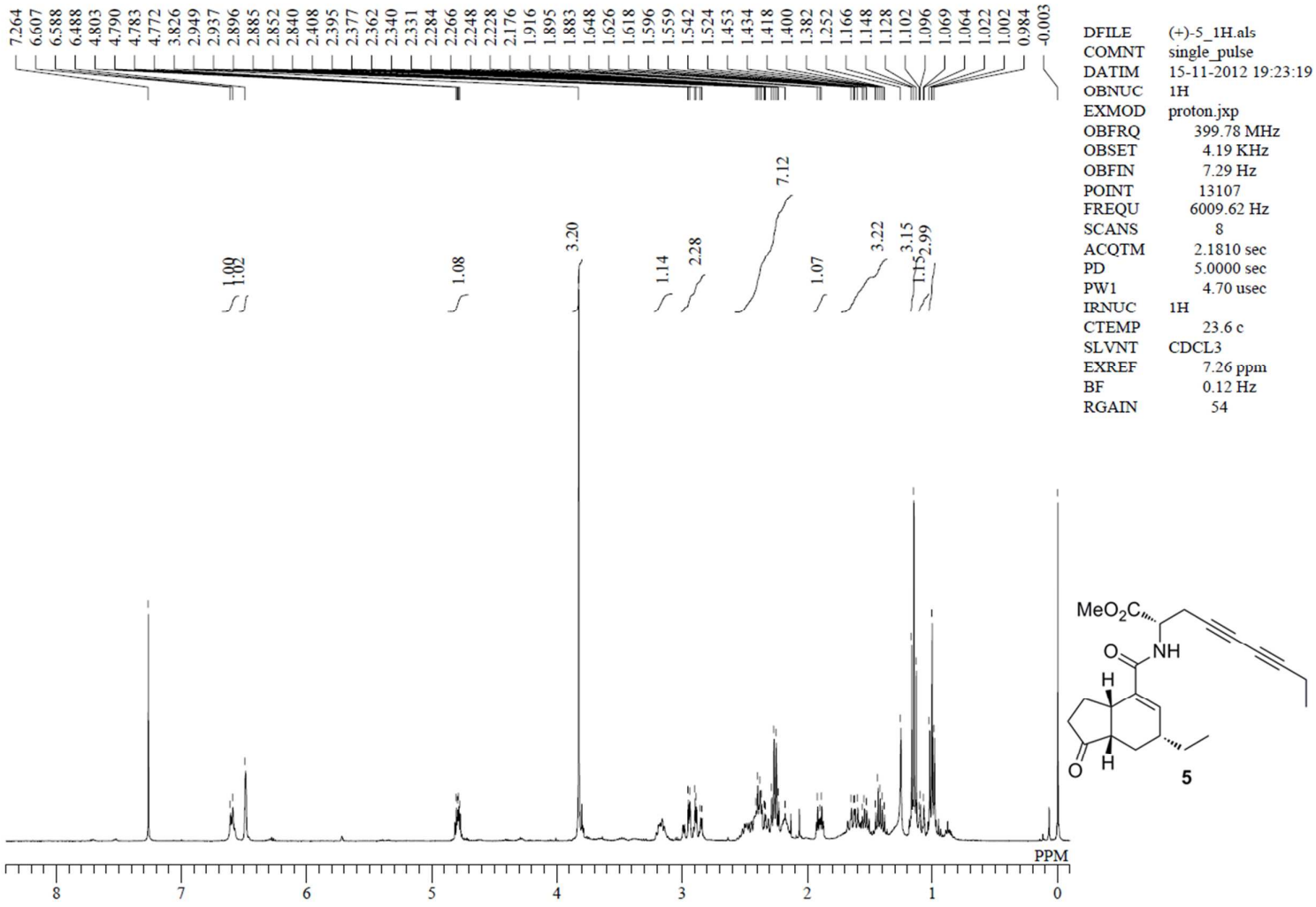
7.264
6.607
6.588
6.488
4.803
4.790
4.783
4.772
3.826
2.949
2.937
2.896
2.885
2.852
2.840
2.408
2.395
2.377
2.362
2.340
2.331
2.284
2.266
2.248
2.228
2.176
1.916
1.895
1.883
1.648
1.626
1.618
1.596
1.559
1.542
1.524
1.453
1.434
1.418
1.400
1.382
1.252
1.166
1.148
1.128
1.102
1.096
1.069
1.064
1.022
1.002
0.984
-0.003
1.00
1.02
1.08
3.20
1.14
2.28
7.12
1.07
3.22
3.15
2.99
DFILE (+)-5_1H.als
COMNT single_pulse
DATIM 15-11-2012 19:23:19
OBNUC 1H
EXMOD proton.jxp
OBFRQ 399.78 MHz
OBSET 4.19 KHz
OBFIN 7.29 Hz
POINT 13107
FREQU 6009.62 Hz
SCANS 8
ACQTM 2.1810 sec
PD 5.0000 sec
PW1 4.70 usec
IRNUC 1H
CTEMP 23.6 c
SLVNT CDCL3
EXREF 7.26 ppm
BF 0.12 Hz
RGAIN 54
MeO2C
O
NH
H
O
H
O
5
PPM
8
7
6
5
4
3
2
1
0

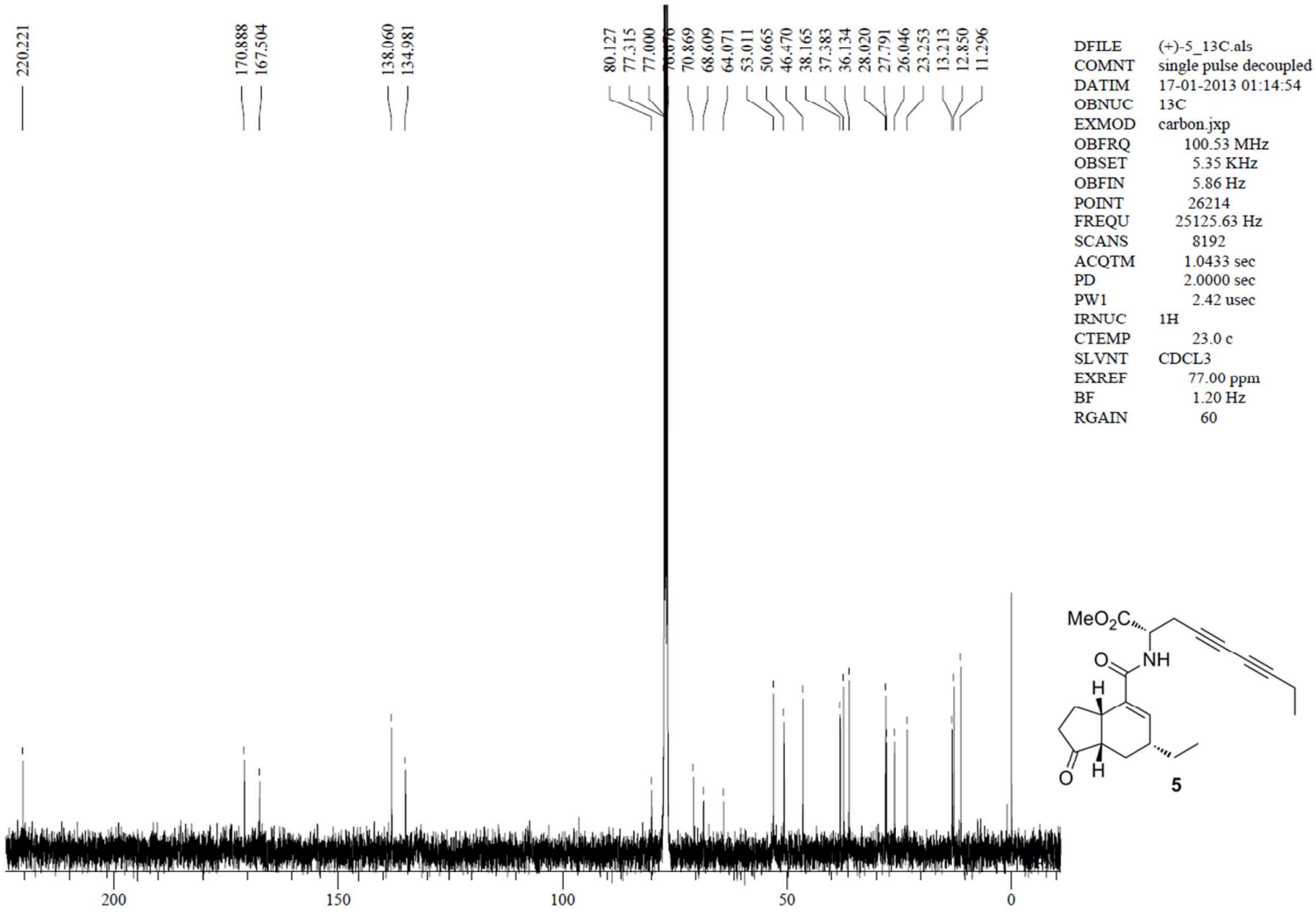
220.221
170.888
167.504
138.060
134.981
80.127
77.315
77.000
70.869
68.609
64.071
53.011
50.665
46.470
38.165
37.383
36.134
28.020
27.791
26.046
23.253
13.213
12.850
11.296
DFILE (+)-5_13C.als
COMNT single pulse decoupled
DATIM 17-01-2013 01:14:54
OBNUC 13C
EXMOD carbon.jxp
OBFRQ 100.53 MHz
OBSET 5.35 KHz
OBFIN 5.86 Hz
POINT 26214
FREQU 25125.63 Hz
SCANS 8192
ACQTM 1.0433 sec
PD 2.0000 sec
PW1 2.42 usec
IRNUC 1H
CTEMP 23.0 c
SLVNT CDCL3
EXREF 77.00 ppm
BF 1.20 Hz
RGAIN 60
MeO2C
O
NH
H
O
H
O
5
200
150
100
50
0

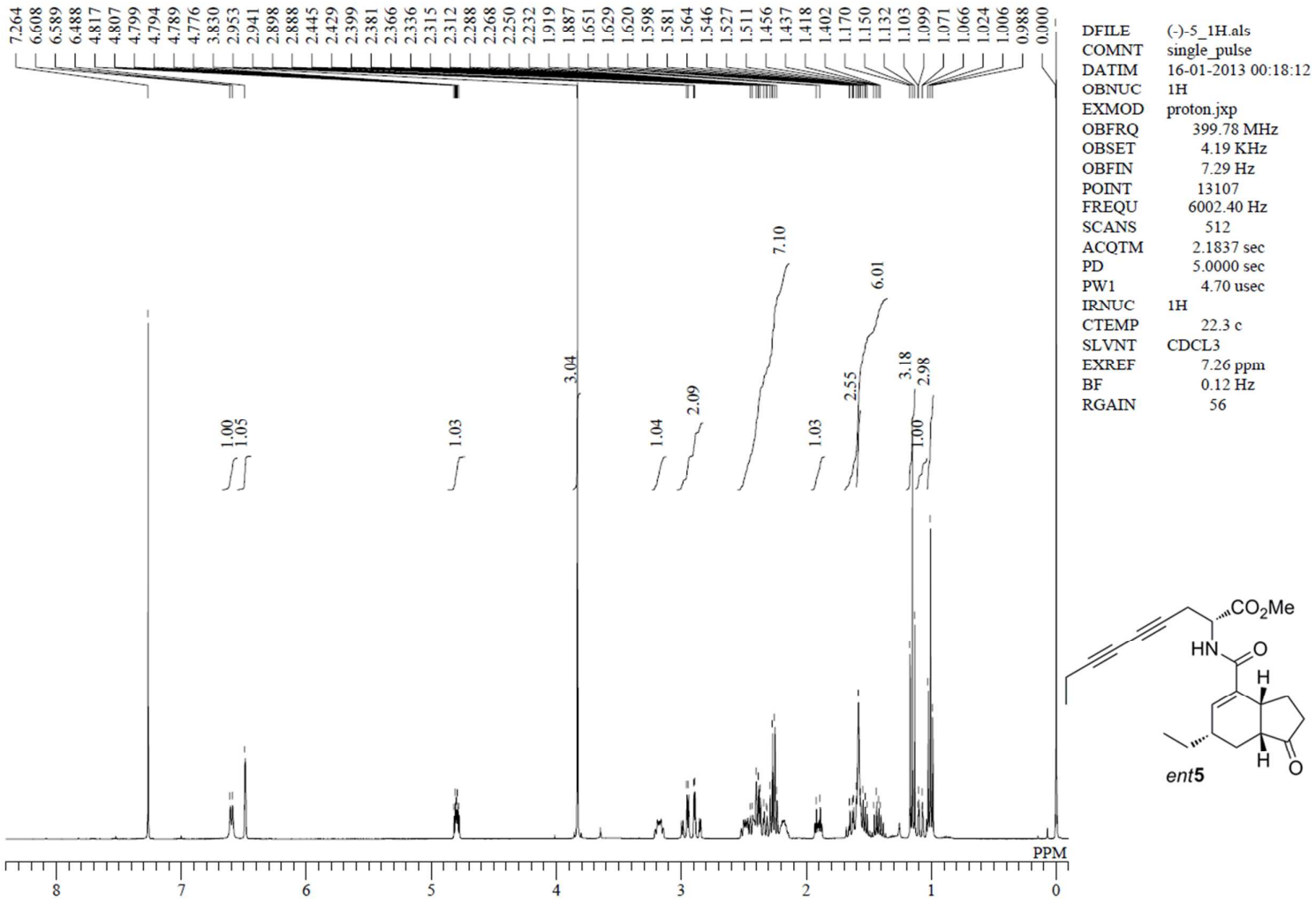
7.264
6.608
6.589
6.488
4.817
4.807
4.799
4.794
4.789
4.776
3.830
2.953
2.941
2.898
2.888
2.445
2.429
2.399
2.381
2.366
2.336
2.315
2.312
2.288
2.268
2.250
2.232
1.919
1.887
1.651
1.629
1.620
1.598
1.581
1.564
1.546
1.527
1.511
1.456
1.437
1.418
1.402
1.170
1.150
1.132
1.103
1.099
1.071
1.066
1.024
1.006
0.988
0.000
1.00
1.05
1.03
3.04
1.04
2.09
7.10
1.03
2.55
6.01
3.18
2.98
1.00
PPM
8
7
6
5
4
3
2
1
0
DFILE (-)-5_1H.als
COMNT single_pulse
DATIM 16-01-2013 00:18:12
OBNUC 1H
EXMOD proton.jxp
OBFRQ 399.78 MHz
OBSET 4.19 KHz
OBFIN 7.29 Hz
POINT 13107
FREQU 6002.40 Hz
SCANS 512
ACQTM 2.1837 sec
PD 5.0000 sec
PW1 4.70 usec
IRNUC 1H
CTEMP 22.3 c
SLVNT CDCL3
EXREF 7.26 ppm
BF 0.12 Hz
RGAIN 56
CO2Me
HN
O
H
H
O
ent5

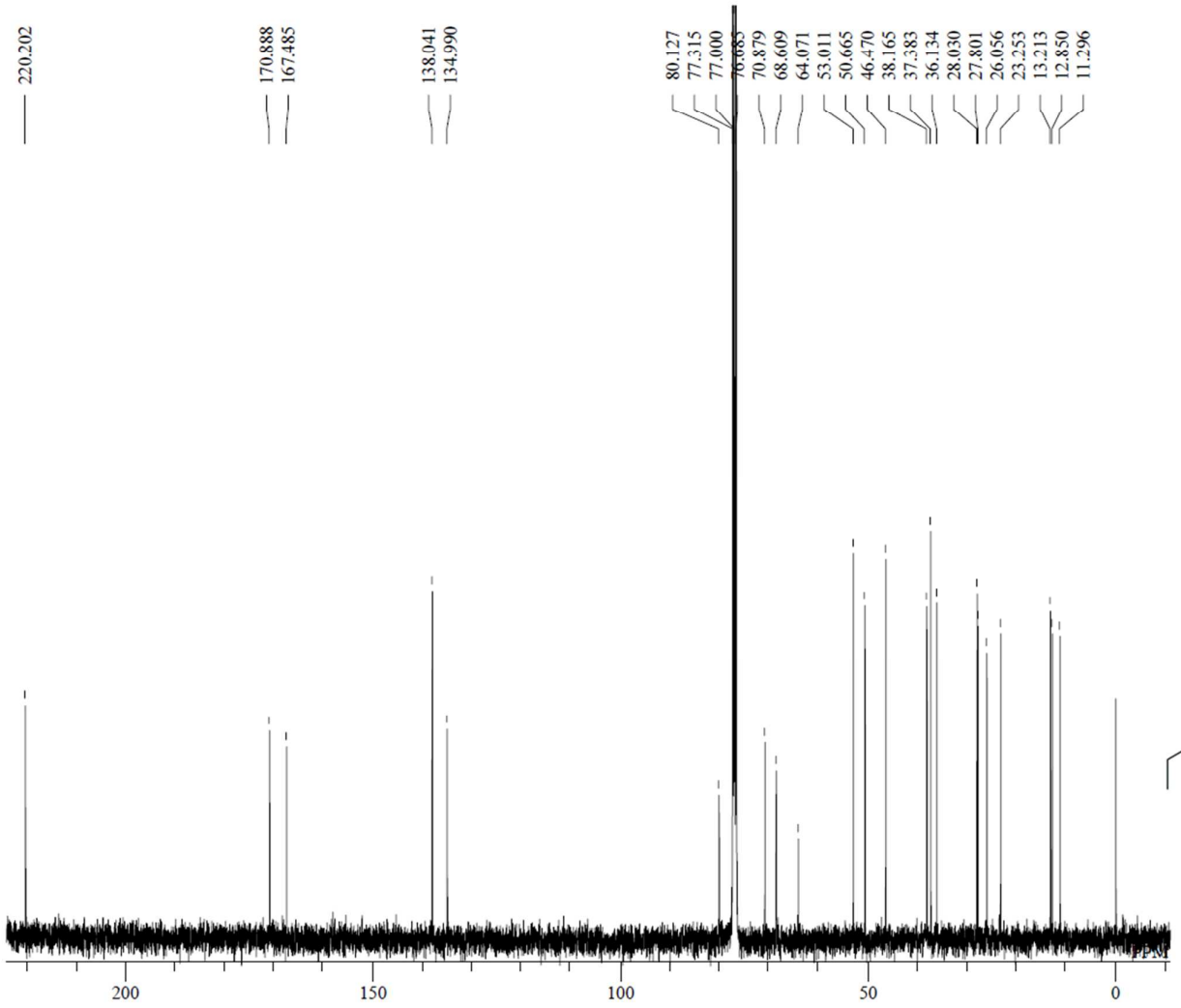

DFILE	(-)-5_13C.als
COMNT	single pulse decoupled
DATIM	16-01-2013 01:22:24
OBNUC	13C
EXMOD	carbon.jxp
OBFRQ	100.53 MHz
OBSET	5.35 KHz
OBFIN	5.86 Hz
POINT	26214
FREQU	25125.63 Hz
SCANS	8192
ACQTM	1.0433 sec
PD	2.0000 sec
PW1	2.42 usec
IRNUC	1H
CTEMP	22.9 c
SLVNT	CDCL3
EXREF	77.00 ppm
BF	1.20 Hz
RGAIN	60

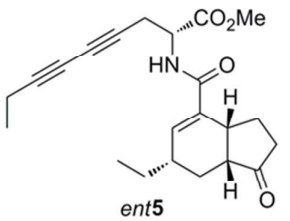

*ent***5**

SI References

43. Nakamura, A.; Takigawa, K.; Kurishita, Y.; Kuwata, K.; Ishida, M.; Shimoda, Y.; Hamachi, I.; Tsukiji, S., Hoechst tagging: a modular strategy to design synthetic fluorescent probes for live-cell nucleus imaging. *Chemical Communications* **2014**, *50* (46), 6149–6152.
44. Manen, H. J.; Kraan, Y. M.; Roos, D.; Otto, C., Intracellular Chemical Imaging of Heme-Containing Enzymes Involved in Innate Immunity Using Resonance Raman Microscopy. *J. Phys. Chem. B* **2004**, *108* (48), 18762–18771.
45. Lieber, C. A.; Jansen, A. M., Automated Method for Subtraction of Fluorescence from Biological Raman Spectra. *Appl. Spectrosc.* **2003**, *57* (11), 1363–1367.